3-1-2024

Introducing pour points: Characteristics and hydrological significance of a rainfall-concentrating mechanism in a water-limited woodland ecosystem

Ashvath S. Kunadi

Tim Lardner

Richard P. Silberstein
Edith Cowan University

Matthias Leopold

Nik Callow

See next page for additional authors

10.1029/2023WR035458

Kunadi, A. S., Lardner, T., Silberstein, R. P., Leopold, M., Callow, N., Veneklaas, E., . . . Thompson, S. E. (2024). Introducing pour points: Characteristics and hydrological significance of a rainfall-concentrating mechanism in a water-limited woodland ecosystem. Water Resources Research, 60(3), article e2023WR035458. https://doi.org/10.1029/2023WR035458

AGU ADVANCING EARTH AND SPACE SCIENCES

Water Resources Research

RESEARCH ARTICLE
10.1029/2023WR035458

Introducing Pour Points: Characteristics and Hydrological Significance of a Rainfall-Concentrating Mechanism in a Water-Limited Woodland Ecosystem

Ashvath S. Kunadi[1], Tim Lardner[2], Richard P. Silberstein[3], Matthias Leopold[2], Nik Callow[2], Erik Veneklaas[4], Aryan Puri[1], Eleanor Sydney[1], and Sally E. Thompson[1,5]

[1]School of Engineering, The University of Western Australia, Perth, WA, Australia, [2]School of Agriculture and Environmental Science, The University of Western Australia, Perth, WA, Australia, [3]School of Science, Edith Cowan University, Perth, WA, Australia, [4]School of Biological Sciences, The University of Western Australia, Perth, WA, Australia, [5]Civil and Environmental Engineering, University of California Berkeley, Berkeley, CA, USA

Abstract The interception of rainfall by plant canopies alters the depth and spatial distribution of water arriving at the soil surface, and thus the location, volume, and depth of infiltration. Mechanisms like stemflow are known to concentrate rainfall and route it deep into the soil, yet other mechanisms of flow concentration are poorly understood. This study characterizes pour points, formed by the detachment of water flowing under a branch, using a combination of field observations in Western Australian banksia woodlands and rainfall simulation experiments on *Banksia menziesii* branches. We aim to establish the hydrological significance of pour points in a water-limited woodland ecosystem, along with the features of the canopy structure and rainfall that influence pour point formation and fluxes. Pour points were common in the woodland and could be identified by visually inspecting trees. Throughfall depths at pour points were up to 15 times greater than rainfall and generally comparable to or greater than stemflow. Soil water content beneath pour points was greater than in adjacent controls, with 20%–30% of the seasonal rainfall volume infiltrated into the top 1 m of soil beneath pour points, compared to 5% in controls. Rainfall simulations showed that pour points amplified the spatial heterogeneity of throughfall, violating assumptions used to close the water balance. The simulation experiments demonstrated that pour point fluxes depend on the interaction of branch angle and foliation for a given branch architecture. Pour points can play a significant part in the water balance, depending on their density and rainfall concentration ability.

Plain Language Summary When rain hits a tree canopy, it either wets the canopy, falls off, or flows along the tree's surfaces (leaves, branches, and trunk). This interaction changes the amount and location of water arriving at the ground. The water flowing underneath branches is may eventually reach the ground by flowing along the tree trunk as stemflow. Using a combination of field observations in seasonally dry Banksia woodlands and rainfall simulation experiments on tree branches, we show that this water may, alternatively, peel off the branch and reach the ground at a "pour point." Rain gauges placed under pour points recorded 1.5–15 times the water recorded at rain gauges under the open sky. We showed that the quantity of water arriving at the pour points varies with the rain volume, and with branch properties including the upstream leaf area, angle, and shape of the branch. The changes in the distribution of water received beneath tree canopies and deeper infiltration into the soil due to pour points proved their hydrological significance. Understanding pour points represents one path toward an improved characterization of the complex processes occurring when rain hits a tree canopy.

Key Points:

- Pour points occur when intercepted rain flowing under tree branches detach and their depths were 1.5–15 times the rainfall
- Pour points increase spatial heterogeneity of throughfall and enhance infiltration into the soil
- Rainfall simulation showed branch structure, foliation, and angle impose unclear controls on the volume of water received at the pour point

Supporting Information:

Supporting Information may be found in the online version of this article.

Correspondence to:

A. S. Kunadi,
ashvath.kunadi@research.uwa.edu.au

Citation:

Kunadi, A. S., Lardner, T., Silberstein, R. P., Leopold, M., Callow, N., Veneklaas, E., et al. (2024). Introducing pour points: Characteristics and hydrological significance of a rainfall-concentrating mechanism in a water-limited woodland ecosystem. *Water Resources Research*, *60*, e2023WR035458. https://doi.org/10.1029/2023WR035458

Received 31 MAY 2023
Accepted 4 FEB 2024

Author Contributions:

Conceptualization: Ashvath S. Kunadi, Nik Callow, Sally E. Thompson
Data curation: Ashvath S. Kunadi, Tim Lardner
Formal analysis: Ashvath S. Kunadi, Sally E. Thompson
Funding acquisition: Sally E. Thompson
Investigation: Ashvath S. Kunadi, Tim Lardner, Aryan Puri, Eleanor Sydney
Methodology: Ashvath S. Kunadi, Tim Lardner, Erik Veneklaas, Sally E. Thompson
Project administration: Ashvath S. Kunadi, Richard P. Silberstein, Sally E. Thompson

1. Introduction

Interception of rainfall by a plant canopy transforms the quantity, spatial distribution (Keim et al., 2005), timing, and momentum of the water fluxes reaching the ground (Ponette-González et al., 2020). The transformations vary with the canopies and with rainfall events for the same canopy (A. Zimmermann et al., 2009). The transformed rainfall fluxes are partitioned into throughfall, free-falling water received beneath a canopy, stemflow, water that runs down the stem (or stems) of a tree, and canopy interception losses, water that never reaches the ground. Throughfall and stemflow play distinct hydrological roles relative to rainfall in vegetated ecosystems (Dunkerley, 2020) which comprise two-thirds of the terrestrial land surface (World Bank, 2022a, 2022b). Given that vegetation growth is strongly related to the presence of rainfall (Lotsch et al., 2003), the canopy interception process is ubiquitous.

Resources: Richard P. Silberstein, Matthias Leopold, Nik Callow, Erik Veneklaas, Sally E. Thompson
Software: Ashvath S. Kunadi
Supervision: Ashvath S. Kunadi, Richard P. Silberstein, Matthias Leopold, Sally E. Thompson
Validation: Ashvath S. Kunadi
Visualization: Ashvath S. Kunadi, Sally E. Thompson
Writing – original draft: Ashvath S. Kunadi
Writing – review & editing: Ashvath S. Kunadi, Tim Lardner, Richard P. Silberstein, Matthias Leopold, Nik Callow, Erik Veneklaas, Aryan Puri, Eleanor Sydney, Sally E. Thompson

Yet an understanding of the mechanisms that transform rainfall into throughfall, stemflow, and canopy interception losses remains incomplete (Allen et al., 2020). Canopies are complex structures, forming "a network of rainfall capturing and conducting channels" (Ford & Deans, 1978). Storage and flow processes on this network govern the partitioning of intercepted water (Whelan & Anderson, 1996; D. F. Levia & Germer, 2015). Describing and defining the flow processes remains a significant gap in hydrological process knowledge (Van Stan et al., 2020).

This understanding is especially important for Mediterranean systems. First, Mediterranean woodlands exhibit the highest variability in rainfall partitioning among biomes globally (see Figure 4.5 in Sadeghi et al., 2020). Second, Mediterranean ecosystems are water limited biomes where the presence of vegetation may increase water losses via interception, or enhance infiltration and suppress baer soil evaporation (S. Thompson et al., 2010). The five regions with a Mediterranean climate receive moderate rainfall (275–900 mm) in the winter and are dry through the summer (Aschmann, 1973). Despite comprising only 2% of the land surface, Mediterranean ecosystems contain some 20% of known vascular plant species (Cowling et al., 1996) adapted to the highly seasonal climate (Veneklaas & Poot, 2003). The flow of rainwater on these diverse plant communities exerts a first order control on the quantum of water available to them during the dry summers (Viola et al., 2008), and the water excesses available to support surface and groundwater resource replenishment (Dralle et al., 2020). Water resource and land management in Mediterranean systems thus require understanding the transformation of rainfall by canopies.

The amount of water that never reaches the ground after being intercepted by trees, canopy interception loss, is a crucial component of the transformed rainfall considered in water resource management. Canopy interception losses are estimated by measuring the water fluxes underneath and above/beside the canopy. These measurements are used to calibrate canopy interception models (Muzylo et al., 2009), used for prediction and in water resources management. Errors in measurement propagate from the event-scale estimates to model parameters. One phenomenon that may contribute to such errors is the extreme spatial heterogeneity in throughfall induced by rainfall interception and redistribution in the canopy (Levia Jr. & Frost, 2006). This heterogeneity is responsible for throughfall depths that range from a fraction of the rainfall depths received to 10 times the depth of event rainfall over a gauge (Cavelier et al., 1997; Holwerda et al., 2006; Lloyd & Marques, 1988; A. Zimmermann et al., 2009). In the Amazonian terra firma rainforest, for example, 29% of 494 throughfall measurements exceeded rainfall and represented 46% of the total throughfall volume captured (Lloyd & Marques, 1988).

Major strides in understanding this spatial redistribution have come from observing throughfall drop size distributions (see Figure 1 in D. F. Levia et al., 2019). A fraction of throughfall drops are "free throughfall," and can be identified by their similarity to rainfall. Once these are accounted for, there are two sets of throughfall drops left. Very small drops are associated with water splashed off from the canopy (splash throughfall), and larger drops are associated with "drip points."

Unsurprisingly, the larger drop sizes of "drip points" generate throughfall in excess of rainfall; not as a total flux, but over a measuring gauge. Drip points were first reported by Rutter, who attributed "unusually high catches" (Rutter, 1963, p. 195) near the stem of *Pinus sylvestris* to "stem-drip" points. The relationship between drop sizes and "catch" would be applicable for differently sized "drip points" as well. Proof that "not all …drip points are equal" (Nanko et al., 2022, p. 5) was found in the drop size distributions beneath foliated and unfoliated trees (see Table 2 in Nanko et al., 2016). Smaller drip points (i.e., smaller drops) were associated with short flow paths over the leaves of trees, and larger drip points (i.e., larger drops) were associated with flow along "woody surfaces." Nanko et al. (2022) distinguished structurally mediated woody surface drip points that were fixed in space from occasional or transient woody surface drip points that moved. The focus of this study on Nanko et al. (2022)'s "structurally mediated woody surface drip points." As we do not measure drop size, we shall identify drip points based on a positively outlying quantity of throughfall compared to rainfall (defined in Section 2.3). We use "drip points" to refer to an outlying reading that are created due to water dripping from a leaf, and "pour points" that are created from a branch. For simplicity, we consider all other forms of throughfall, that is, splash throughfall and free throughfall, as simply "throughfall", and return to the issue of classification and nomenclature applied to canopy flow processes in the Discussion.

We hypothesize that pour points could play an important hydrological role. Pour points are expected to (a) increase the heterogeneity of throughfall (Stan et al., 2020) by redirecting water from other parts of the canopy and (b) enhance throughfall recorded at the pour point. We expect both these processes would complicate the measurements of fluxes to the land surface water balance and increase the infiltration of water into the soil.

Throughfall (along with drip and pour points) is usually the greatest flux to the land surface below vegetation (Sadeghi et al., 2020). Standard throughfall sampling designs (Genton, 1998; Kimmins, 1973; A. Zimmermann & Zimmermann, 2014) rely on the coefficient of variation (CV). This can inform the sampling design through an assumption of normality. Increasing the heterogeneity of throughfall increases the CV and increases the sampling requirements. Redirecting rainfall to a point would, also, create an outlier in the throughfall distribution. This would contaminate the assumption of normality, and need additional statistical treatment (A. Zimmermann & Zimmermann, 2014). Additionally, the detachment of the water flowing under the branch reduces the stemflow flux (as had the water not detached it would have formed a part of stemflow). Therefore, if pour points are present and not measured, interception losses will be overestimated, based on the water balance assumption.

Guswa and Spence (2012) predicted that groundwater recharge would increase with the spatial heterogeneity of water arriving at the soil surface. These predictions were shown to be true in dye experiments, where accelerated infiltration was seen under vegetated canopies (van Meerveld et al., 2021). By increasing heterogeneity, pour points could similarly increase infiltration. Apart from increasing the spatial heterogeneity, pour points create an outlier in the flux of water to the land surface. A similar outlier in water flux is created by stemflow, that is associated with the "double-funneling" phenomenon (Johnson & Lehmann, 2006). The first funnel is the one formed by the canopy of the tree, as it channels the water from the extremities of the canopy to the stem. This water infiltrates deeper along the second, inverted, funnel formed by the root system, as it redirects the water along the existing root pathways (Liang, 2020). This water has a disproportionate importance for soil water and groundwater (Návar, 2011; Nulsen et al., 1986). For example, stemflow was only 0.5%–1.2% of rainfall but supplied nearly 20% of the recharge flux in measurements in a Japanese pine forest (Taniguchi et al., 1996). Pour point water fluxes are even more localized as areal extent around the circumference of a stem is considerably greater than a drop. Consequently, they may similarly have a subsurface fate that is distinct from rainfall and throughfall.

The enhanced infiltration effects may be exacerbated as pour points drops are larger (D. F. Levia et al., 2017) with greater kinetic energy than rainfall, creating larger craters in the soil than throughfall (Beczek et al., 2018; Mazur et al., 2022), promoting infiltration (S. E. Thompson et al., 2010). Splash from droplets may also remove surface litter or hydrophobic layers (Lowe, 2019). The deeper water infiltrates during storms, the more likely it is to evade rapid soil evaporation (Or & Lehmann, 2019).

There is sparse literature to consider in designing this study to investigate pour points. However, studies on stemflow may be leveraged as it emerges from flow along branches in the canopy. The only physics based model of stemflow (Tucker et al., 2020) was developed to describe the flow within furrows of tree bark. This model, however, ignores the effects of surface tension, that are an important consideration for pour points. Experimentally, stemflow initiation occurs either when rainfall is intercepted by a branch (Alshaikhi et al., 2021; Herwitz, 1987) or is intercepted by leaves and then drains onto the branch. Both pathways wet the branch. Once the upper half of the branch is wet (Bulcock & Jewitt, 2010), water flows to its underside, forming a hanging or pendant rivulet (Alekseenko et al., 2008; Indeikina et al., 1997) which then flows downgradient beneath the branch. Rivulets that detach before reaching the stem form a pour point, and rivulets reaching the stem form stemflow (Herwitz, 1987). This is discussed from the perspective of drop sizes by Nanko et al. (2022).

Laboratory and field studies have linked increased stemflow volumes to greater branch inclination above horizontal (Bialkowski & Buttle, 2015; Crockford & Richardson, 1990; D. Levia et al., 2015; D. F. Levia & Germer, 2015; Martinez-Meza & Whitford, 1996; Van Elewijck, 1989), and higher leaf area (Staelens et al., 2011). However, neither of these observations is universal (Garcia-Estringana et al., 2010; Iida et al., 2021; D. F. Levia & Germer, 2015). There is also experimental evidence for an increase in drop size recorded underneath the canopy in the absence of leaves (Nanko et al., 2016, 2022), which may indicate higher rates of pour point formation. It is evident that a relationship exists between canopy architecture and pour point formation, and canopy redistribution of rainfall in general, but the nature of this relationship is still unclear.

We aim to extend investigations of pour points by combining field observations in a water-limited seasonally dry (Banksia) woodland ecosystem with rainfall simulation experiments on branches from the co-dominant canopy species, *Banksia menziesii*. In this study, we look at gross storm or simulation scale characteristics to address four basic research questions:

1. Can pour points be identified in the Banksia woodland?
2. Could the magnitude and fate of pour point fluxes be hydrologically relevant?

3. What are the implications of pour point formation for measuring throughfall and closing the canopy water balance?
4. How do storm depth, branch foliation and angle influence the flux of water through pour points?

2. Methods

2.1. Field Site

Field observations were made at the Gingin Ozflux Supersite (Beringer et al., 2022), a Mediterranean woodland ecosystem in the southwest of Western Australia (GPS coordinates: 31°22′35.04″S, 115°42′50.04″E; elevation: 51 m). The site overlies the Gnangara groundwater mound, an important but declining (Ali et al., 2012) groundwater resource for the city of Perth (Skurray et al., 2012). The site has a warm Mediterranean climate, with an annual rainfall of approximately 680 mm/year, most of which falls between May and October. The annual mean temperature is ≈18.5°C, with hot summers and mild winters. Soils are deep, coarse, nutrient-depleted sands with low relief (Salama et al., 2005; Turner & Laliberte, 2020). The organic surface horizon is often extremely hydrophobic (Lowe, 2019), becoming less so as soils wet during winter. Hydrophobicity creates strong preferential flow paths, alters soil evaporation, and generates spatially heterogeneous patterns of wetting (Rye & Smettem, 2017). The soil is overlain by a canopy of leaf area index 0.7–0.9 (Beringer et al., 2016). The stem density is roughly 386 trees per hectare with an average basal area of 9.87 m^2 ha^{-1}. The height of the canopy is 6.8 m; as assessed visually when climbing a vertical tower. *Banksia menziesii* is the dominant canopy species comprising 60% of the trees, with the similar *Banksia attenuata* representing most of the remainder of the canopy (33%), with infrequent *Eucalyptus todtiana* (3%).

The Gingin Ozflux site contains significant infrastructure installed through Australia's National Collaborative Research Infrastructure Strategy (NCRIS) Terrestrial Ecosystem Research Network (TERN) program, to measure water fluxes in the Banksia woodland (Silberstein, 2015). Existing infrastructure includes a throughfall gauge network consisting of 32 Nylex 250 mm Professional Rain Gauges ("manual gauges") and 10 statically calibrated Davis 7852M tipping-bucket automatic rain gauges (ARG1s). The gauges are arranged in two fixed square arrays consisting of 16 manual gauges and 5 ARG1s each (see green circles and triangles in Figure 2a). In each square array, the manual gauges are arranged in an evenly spaced grid of 30 m by 30 m, and the ARG1s are placed in an "X" shape within the square arrays (see green triangles in Figure 2b). Rainfall is measured in co-located manual and continuously-recording ARG1s at 3 open sites (1 shown in Figure 2a).

We developed a methodology to identify pour points below Banksia branches in this woodland (using observations during rain events, example in Supporting Information S1). Given the structurally mediated nature of these points (Herwitz, 1987; Nanko et al., 2022), we expect pour points to form at locations where the water flowing under a branch exceeds the branch's carrying capacity, as illustrated in Figure 1a). This can occur at (a) a convergence of branches (Figure 1b) where there is a confluence of two or more streams or (b) a change in branch angle (Figure 1c) where the branch carrying capacity is reduced. Additional indicators of pour points included high leaf area, smoothing and discoloration of the bark on the underside of branches, and splash marks on the sand, similar to the ones observed by Geißler et al. (2012), after a rain event. We used these features to identify potential pour point locations, focusing on an area close to the permanent throughfall sensor grids (see Figure 2a). We surveyed the location of all confirmed pour points in this area using a total station, allowing us to estimate the spatial density of pour points within the polygon highlighted in yellow in Figure 2a).

2.2. Field Instrumentation

We installed manual gauges under potential pour points (pour point gauges), and under branches where some but not all canopy features indicated a pour point could form (negative test gauges) for both *B. menziesii* and *B. attenuata*. If pour points were confirmed via manual gauges, they could be replaced with a statically calibrated tipping bucket rain gauge (Davis AeroCone Rain Collector with Flat Base for Vantage Pro2 - ARG2). In September 2020, we placed manual rain gauges under a *B. menziesii* tree, targeting two pour points under a single branch and a negative test gauge on a neighboring branch. Between March and May 2021, 14 additional manual pour point gauges and 4 negative test gauges were installed under other trees. In July 2021, the manual gauges under the original two pour points (PPCT and PPFT in Figure 5b) were replaced with ARG2s, and a stemflow collection system was fitted with an ARG2. Note that the depth from the different gauges (stemflow, pour point, throughfall, and rainfall) were calculated using the ratio of the volume of water collected in the gauge and the area

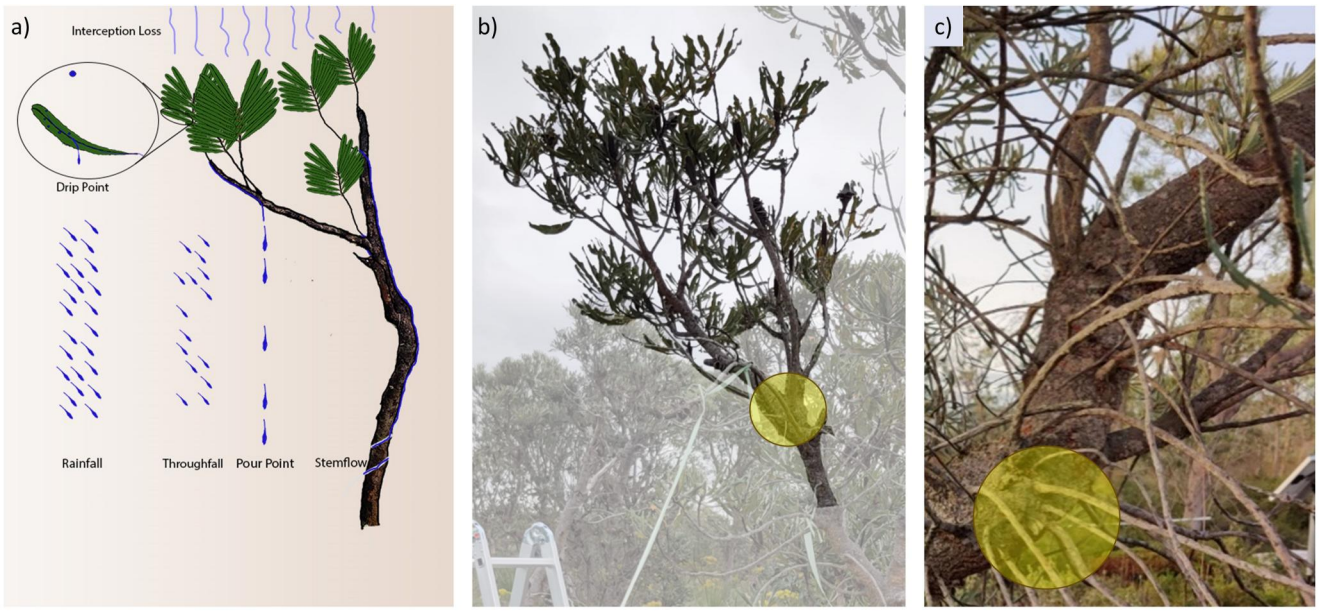

Figure 1. Partitioning of rainfall by a canopy and the canopy features that provide visible indicators of pour point presence. (a) Rainfall intercepted by canopies is partitioned into interception loss (evaporation), throughfall, stemflow and pour points fluxes. Pour points are generated at visually identifiable features of the canopy including (b) the confluence of smaller branches or (c) a change in branch angle. The location where we expected the pour point to form is highlighted with yellow circles in (b) and (c).

of the gauge. This methodology was chosen as we could not ascertain the crown area contributing water to the pour points. Two manual gauges under a *B. attenuata* (NDP8 and NDP9 in Figure 5b) were also replaced with ARG2s. The instrumentation types and dates in the field are summarized in Table 1.

In June 2021, we installed calibrated soil moisture sensors (Delta-T-Device Thetaprobe Ml2x, and Campbell Scientific CS650 Soil Water Content Reflectometer sensors) below three trees. Sensors were installed while

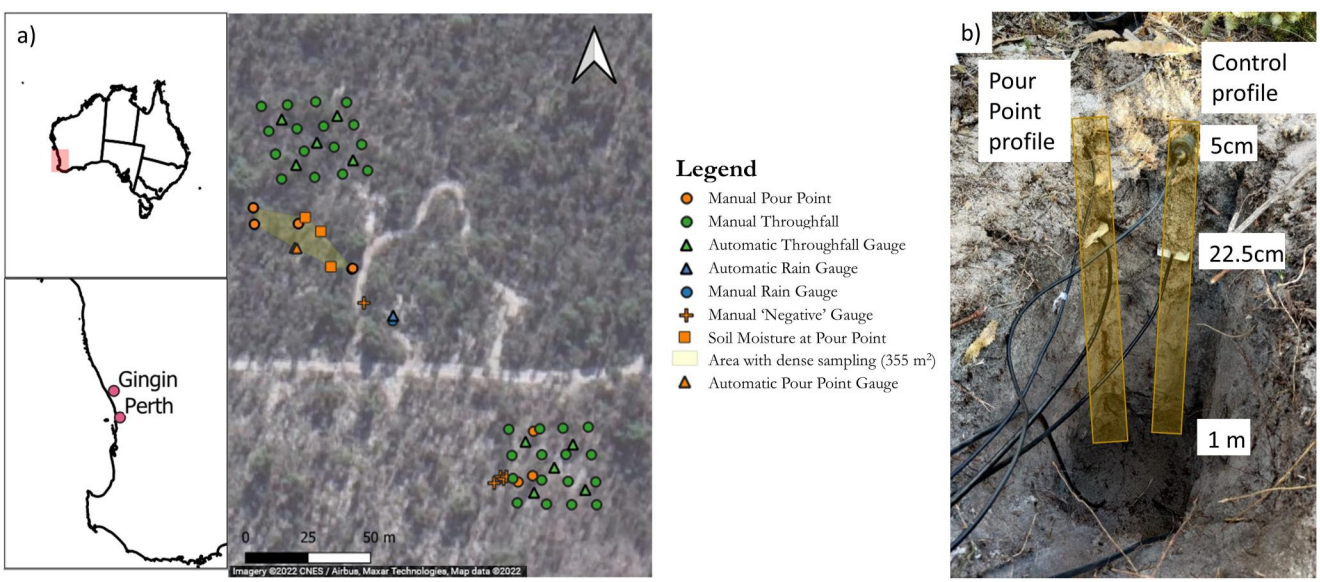

Figure 2. (a) The site map of relevant instrumentation at TERN Ozflux Gingin Supersite overlain on Satellite Imagery. There was an additional tree instrumented further north where PPCT, PPFT, and Control were located as written in Table 1. Some of the trees had more than one pour point instrumented making them harder to discern at this scale. (b) Shows the soil moisture instrumentation that was placed once a pour point was confirmed (indicated with an orange square in the map), the right side probes were the control profile and the left side has the pour point instrumented.

Table 1
Pour Point Instrumentation Details

Field code	08/09/2020	05/03/2021	23/04/2021	21/05/2021	28/05/2021	03/06/2021	16/06/2021	08/07/2021	17/03/2022	24/06/2022
PPCT	Installed						ARG2		Branch Cut	Removed
PPFT	Installed						ARG2		Branch Cut	Removed
Control	Installed								Branch Cut	Removed
NDP1		Installed	Shifted	SM Sensors						
NDP2		Installed		Removed	SM sensors					
NDP3		Installed								ARG2
NDP4				Installed		SM sensors				
NDP5				Installed		SM sensors				
NDP6				Installed						
NDP7				Installed						
NDP8				Installed			ARG2			
NDP9				Installed			ARG2			
NDP10				Installed						
NDP11								Installed		ARG2
NDP12								Installed		ARG2
SDP1[a]		Installed	Removed					Installed		
SDP2[a]		Installed								
SDP3		Installed	Removed					Installed		
SDP4								Installed		
SDP5								Installed		
SDP6								Installed		
SDP7								Installed		
SFGB							ARG2			Removed

Note. The NDP and SDP are part of the Northern Dense Points and Southern Dense Points, indicating where these points were located close together in a cluster. Installed - a manual rain gauge was placed under the point. ARG2 - the manual gauge was removed from the point and an ARG2 was placed. SM sensors - the manual gauge was removed from the point and soil moisture sensors were installed along the vertical profile under the point. Branch cut - A branch that was surveyed at the site was cut and taken for rainfall simulation experiments. Removed - the sensor was removed. [a]SDP1 and SDP2 were not put in the field for the duration indicated by the time interval between the date of removal and the second installation date.

keeping their rods horizontal, using access trenches, at depths of 5 cm, 22.5 cm, and 1 m beneath confirmed pour points, and at control locations approximately 20 cm away. We positioned the middle of the sensor probes to be under the pour point and aligned the probes with the branch. The control soil moisture probes were oriented perpendicular to the branch. The installation under one pour point is shown in Figure 2b.

The 5 cm deep sensors were intended to identify if the pour point was contributing water to the soil profile. We estimated beneath a depth of 22.5 cm, water would be hydraulically disconnected from the sandy soil surface and, therefore, not be subjected to rapid (Stage 1) soil evaporation (Or & Lehmann, 2019). Finally, 1 m is the estimated rooting depth of approximately half of the shrub species in the Banksia ecosystem (Groom et al., 2000) so that water passing below this point is inaccessible to understorey vegetation.

Data were collected from August 2020 until June 2022. Power outages were caused by the disconnection of the batteries from the solar panels (likely by kangaroos) and battery theft. This caused data unreliability and loss - these were manually filtered out. One soil moisture sensor (a control) failed and data were replaced by the average of the other control sensors for the same depth during the period of failure. The ARG2s would routinely clog with what looked like bark material. The events when the data under the pour point was decoupled from rainfall trends, that is, a smooth increase in rainfall depth rather than the characteristic jagged increase, were manually filtered out.

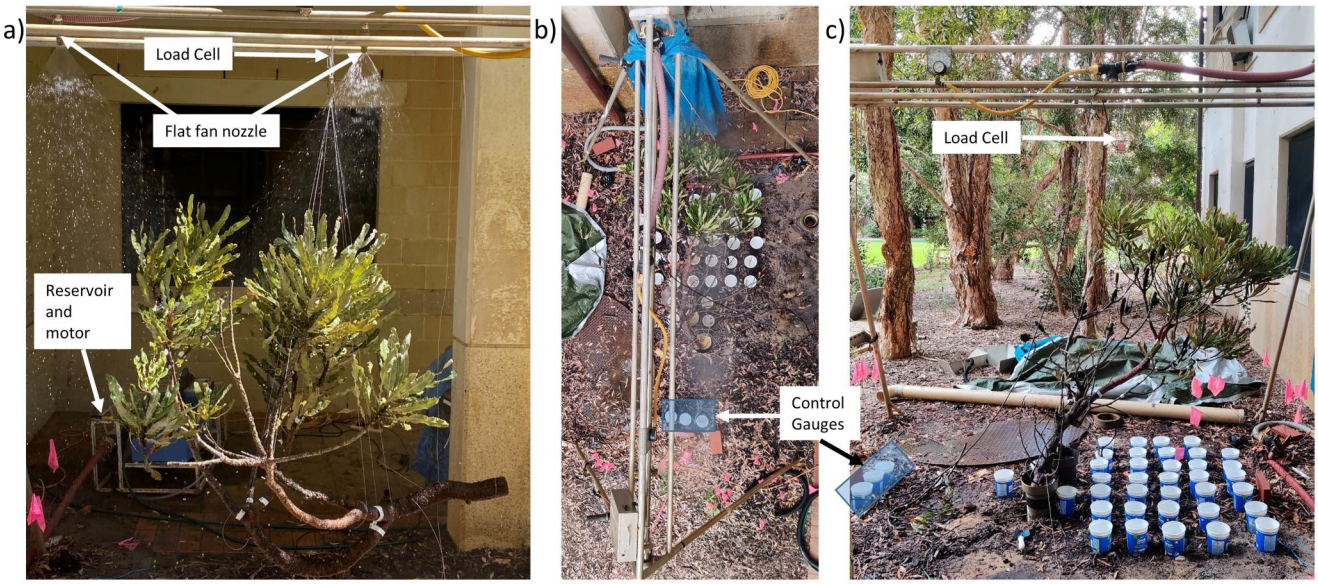

Figure 3. Rainfall simulation experiments. (a) *Br*1 with the rainfall simulator operational hanging from the load cell using a fishing line. *Br*1 did not need a gauge to measure the stemflow as all the water was being drained at the bottom of the U-bend of the branch. (b) The plan view of the rainfall simulator with the throughfall arrangement. (c) Gingin branch was monitored in the field and then was brought to the simulator, as shown in the image, with the end of the branch going into a tipping bucket rain gauge for stemflow measurement. Three throughfall buckets separated from the rest of the gauges are marked as the control buckets in (b) and (c). They are not influenced by the branch and allow comparisons between trials.

2.3. Rainfall Simulations

We conducted rainfall simulator experiments on five *B. menziesii* branches with a consistent rainfall intensity. We selected four test *B. menziesii* branches and one control branch from the Gingin site and the University of Western Australia Shenton Park Field Station (31°56′53.80″S, 115°47′39.69″E). One of the branches (the Gingin branch, *GBT*, shown in Figure 3c) was removed from Gingin after ≈18 months of field monitoring.

The in situ angle of each branch was measured with an inclinometer. This was measured at the closest straight section (long enough to fit the inclinometer) to where the branch was to be cut. This was different for each branch due to the peculiarities in the branch architecture. The branch was cut and the cut end was wrapped in a wet towel and a heavy-duty garbage bag before the whole branch was wrapped in a tarpaulin and transported to a cool room (4°C). The branch was then taken out once to be photographed. It was then placed back in the cool room before being used in the rainfall simulator experiments. All experiments were conducted within a 3-day period. The *B. menziesii* leaves are thick and tough and stayed green during the 3 days. Additionally, these leaves don't change shape or wilt when drying, making them suitable for such experiments.

Rainfall simulations were run outdoors in a sheltered courtyard area (see Figure 3). The simulator drew water from a 60 L reservoir with a fixed displacement pump. Water was piped to a rotating arm with three replaceable flat fan nozzles and a pressure gauge. The nozzle arm was connected to a programmable motor that controlled the simulation area by limiting the angles up to which the nozzle arm rotated. Using an 80-20 flat fan nozzle (the smallest available), the simulator applied approximately 15 L/min over a 2.5 m × 0.6 m area. This corresponds to very heavy rainfall ≈190 mm/hr, with a spatial uniformity coefficient (Christiansen, 1942) of 87%. This is not representative of the rainfall events observed in the field, and it would have been desirable to further restrict the simulator's output, however, this rate was the minimum we could achieve with our equipment.

Branches were suspended from a calibrated Bonhshin DBBP S-beam 20 kg load cell (Loadcell Supplies, 2010) which was logged continuously during experiments at 1-s intervals with a Campbell Scientific CR10x. Manual rain gauges (10.8 cm diameter) were placed in a regular grid beneath the simulator. A 20 cm × 30 cm grid was used for the first branch (*Br*1) and a 10 cm × 30 cm grid was used for all other branches. One Texas Instruments TR-525USW Tipping Bucket Rain Gauges (ARG3s) was positioned at the end of the branch to capture "stem-flow" (when it was present) and another beneath the pour point. Data from the load cell and ARG3s were logged

with the CR10x at 1-s intervals. At the end of each experiment, we measured the volume of water in each manual gauge and converted this to an equivalent depth. Rainfall simulations were run for 15 min or until any manual rainfall gauge was almost full.

We ran experiments on each branch when it was wet and dry, and for at least three different branch angles once it was wet. We then removed one third of all leaves and repeated the experiments and defoliation for branches with 100%, 67%, 33%, and 0% foliation. In all, 93 rainfall simulation experiments were conducted. For each of these 93 experiments, we measured the water volume in the manual gauges, the mass on the load cell, and flow rates from the pour point/stemflow flows.

2.4. Data Analysis

All analyses were conducted in R version 4.0.0 (R Core Team, 2018). "dplyr," "reshape2" (Wickham, 2007), "strucchange" (Zeileis et al., 2002), and "lubridate" (Grolemund & Wickham, 2011) packages were used for data analysis. "ggplot2" (Wickham, 2016), "ggextra," "virdis" (Garnier et al., 2021), and "scales" packages were used to plot the results. QGIS 3.14.16-Pi (QGIS Development Team, 2022) was used to make the map in Figure 2a.

2.4.1. Field Data

2.4.1.1. Pour Point Identification and Fluxes

We defined rainfall "events" as periods of rainfall separated by at least 2 hr of no rainfall. We classified measured throughfall as a pour point if there was at least 1.5 times and the water could be reasonably posited as coming from a branch. The comparison was done over an event for ARG1s, or over cumulated events for manual gauges. We arrived at the value of 1.5 via a statistical analysis of throughfall in the rainfall simulator experiments (see Section 2.4.2 below). The identified pour point locations were used to address Research Question 1. Once identified, we compared pour points to stemflow or throughfall based on the ratio of the fluxes normalized by gauge area. The normalized fluxes at the pour points and their magnitude relative to rainfall, stemflow, and other throughfall provide answers to Research Question 2. Finally, we linked storm characteristics to pour points by regressing the average pour point depth (across ARGs) against rainfall depth for each storm and applied a breakpoint analysis (Zeileis et al., 2003), and used the results to partly address Research Question 4.

2.4.1.2. Soil Moisture Data Analysis

We analyzed the soil moisture data at event and seasonal timescales. On event timescales, all readings were initialized to reflect event-based changes to the soil moisture, by subtracting initial soil moisture $SM_{s,d,e}[t=1]$ for each sensor profile location s, depth d and event e from all measurements after the event started ($t>1$). We termed this event soil moisture or $ESM_{s,d,e}[t]$. To assess the excess water that has passed through the soil moisture sensor at any time step, we applied a difference detrending filter (Eroglu et al., 2016) which subtracts soil moisture measurements for consecutive points in time:

$$\Delta ESM_{s,d,e}[t] = ESM_{s,d,e}[t] - ESM_{s,d,e}[t-1] \tag{1}$$

Next, to assess the changes between control and the pour point soil moisture sensors during an event, we subtract $\Delta ESM_{s,d,e}[t]$ observed at pour point and at its associated control soil moisture sensors:

$$DESM_{pp,d,e}[t] = \Delta ESM_{pp,d,e}[t]|_{pp} - \Delta ESM_{pp,d,e}[t]|_{control} \tag{2}$$

where, the suffix *pp* and *control* refer to neighboring pour point and control sensors at *pp* and depth d. On seasonal timescales, we calculated the infiltration for each sensor location (I_s) profile by:

$$I_s = \sum_{e=1}^{e=N}\left(\sum_{d=1}^{d=3}\left(z \times \sum_{t=1}^{t=T}(\Delta ESM_{s,d,e}[t])\right)\right) \tag{3}$$

where, T represents the time taken for event e, N represents the number of events, and the d index goes through the three depths measured. The product of event wise sum across a depth (z) represented by each sensor (defined by

the midpoint between sensors/the domain boundary of 0–100 cm) provides an estimate of the total depth of water infiltrated for that event. The summation across all the events represents the infiltration for the season.

2.4.2. Rainfall Simulator Data

2.4.2.1. Normalization and Calibration

Because rainfall simulations ran for different durations and may have a drop in pressure due to human error, all measured depths were normalized to create $ND_{i,g}$, where i represents the trial number and g represents the gauge position. This was done by dividing the depth in all gauges ($D_{i,g}$) by the mean depth of water in the three control gauges $\left(\overline{D}_{i,cg}\right)$, seen in Figure 3, for each trial. $\overline{D}_{i,cg}$ was seen to vary with the simulation duration in cases when the pressure had been maintained consistently during the simulation.

To create a background rainfall field without branches, we computed the normalized rainfall in 19 calibration trials, moving the ARG3s for each trial. These data formed a calibration dictionary where the normalized, background rainfall without the branch $ND_{cal,g,j}$ was known for any gauge location g and ARG3 position j. We used the ratios of $ND_{i,g}$ and the corresponding $ND_{cal,g,j}$ to estimate the ratio of throughfall, pour point, or stemflow fluxes to background rainfall.

2.4.2.2. Identifying Pour Points

We used a robust outlier identification approach (B. Zimmermann et al., 2010) to find gauges with anomalously high throughfall based on the z-score (Rousseeuw & Hubert, 2011):

$$z_i = \frac{x_i - \tilde{x}}{1.483 \times \widetilde{|x - \tilde{x}|}} \tag{4}$$

where the $\sim$ indicates the median operator, and where x, in this application, represents the ratio of normalized throughfall to background rainfall for each gauge. Outliers have $z > 2.5$. The minimum ratio of throughfall to rainfall producing $z \geq 2.5$ using data from all 93 trials was 1.5, the same threshold used to identify pour points in field data.

2.4.2.3. Storage of Water on the Branch

For each trial i, we identified the time rain started (t_s), the initial branch weight (W_i), the time the branch reached its maximum weight (t_{eq}) and mass of water on the branch at that time (ΔW_{mx}), the timing of rainfall cessation (t_e), the weight loss after rapid drainage ($W_{t=t_{de}}$) and the final branch weight W_f by fitting a piece-wise function to the load cell data. The structure of the piece-wise function was (Keim et al., 2006):

$$|W(t)| = \begin{cases} W_i & t < t_s \\ W_i + \Delta W_{mx} \times \left(1 - e^{-\frac{(t-t_s)}{RF}}\right) & t_s \leq t < t_e \\ W_i + \Delta W_{mx} \times \left(e^{-\frac{(t-t_e)}{FF}}\right) & t_e \leq t < t_{de} \\ W_f + \left(W_{t=t_{de}} - W_f\right) \times \left(e^{-\frac{(t-t_{de})}{EVF}}\right) & t \geq t_{de} \end{cases} \tag{5}$$

The piecewise function separates rising, falling and evaporating sections and quantifies the parameters RF, FF, and EVF that describe the corresponding mass changes. We refer to the mass of water on the branch at the end of the falling limb as the branch storage (Aston, 1979; Li et al., 2016). This nomenclature differs from some other studies (Keim et al., 2006; Xiao & McPherson, 2016) that use ΔW_{mx} as branch storage.

2.4.2.4. Mass Balance and Throughfall Heterogeneity

The total rainfall applied, the total throughfall collected, and the storage measured on the branch allow the water balance for each trial to be assembled as:

$$W_{t=t_{de}} - W_i = \frac{A_{sim}}{\sum A_g}\left(\overline{D}_{i,cg} \times \rho_{water} \times \sum((ND_{cal,g,j} - ND_{i,g}) \times A_g)\right) + \epsilon \quad (6)$$

where A_g is the surface area of a gauge, A_{sim} is the area under the rainfall simulator (1.5 m^2), ρ_{water} is the density of water and ϵ is the water balance residual (error). We computed error for three kinds of throughfall estimates - (a) when using throughfall measured in all gauges, (b) excluding pour point and stemflow gauges, and (c) excluding all identified outlier gauges, to answer research question 3.

To complement the mass balance estimates, we computed the number of samples needed to estimate the mean throughfall each of these three throughfall estimates, using Kimmins (1973):

$$n_c = \left(\frac{t \times \sigma}{c \times mean}\right)^2 \quad (7)$$

where n_c is the number of collectors required for a given confidence c around the *mean* of the throughfall readings for a given standard deviation σ, and t is Student's t value. Although this design approach is strictly valid only for normally distributed and spatially independent measurements of throughfall, it offers an easily interpreted indicator of the impact of pour points on throughfall sampling requirements. Additionally, it shows the strain imposed on conventional techniques when pour points are considered the same as throughfall.

The mass balance residual and the estimated sampling requirements from the rainfall simulator experiments were used to answer Research Question 3.

2.4.2.5. Branch Angle and Foliation Effects on Pour Point and Stemflow Fluxes

The concentration of rainfall by the pour point ($ND_{i,g=pp}/ND_{cal,g=pp,j}$) and stemflow ($ND_{i,g=sf}/ND_{cal,g=sf,j}$) were compared as a ratio. Additionally, we visually and statistically explored how concentration at pour point and the ratio of pour point to stemflow concentration varied with branch angle and foliation for each branch to answer Research Question 4, using simple linear models of the form:

$$\Delta \frac{ND_{i,g=pp}}{ND_{cal,g=pp,j}} \approx \beta_0 + \beta_1\alpha + \beta_2 f + \beta_3 f \times \alpha, \quad (8)$$

where $\Delta \frac{ND_{i,g=pp}}{ND_{cal,g=pp,j}}$ is the deviation of the ratio of pour point depth to precipitation depth from its mean (calculated for all simulations for a branch), f is the degree of branch foliation, and α is the deviation of the branch angle from its mean (calculated for all simulations for a branch). Similar models were also run for the ratio of pour point to stemflow concentration.

3. Results

3.1. Research Question 1: Can Pour Points Be Identified in the Banksia Woodland?

We defined a pour point as a location on a branch under which water received is ≥1.5 × rainfall at least for one event. This means that a pour point location might get less than this limit for some events due to insufficient rain. Using this definition, 15 of 16 of suspected pour point locations and 1 of 6 "negative" test locations (seen in Figure 4) were classified as pour points. The false negative occurred at a site where we considered the change in angle to be insufficient to induce a pour point. We could not explain the cause of the false positive.

Incidentally, 1 of the 10 ARG1s in the throughfall grid was identified as measuring a pour point. This will be referred to as the "IncidentalPP" in Figure 5. We verified that the canopy above the ARG in the throughfall grid contained a curved *B. menziesii* branch. Figure 1a was inspired by the pour point of this tree.

The four test branches visually identified as being likely to form pour points in the rainfall simulator all did so. A sample rainfall simulation with a pour point can be seen in Movie S2. The control branch (*Br*3) did not form pour points (see Table 2).

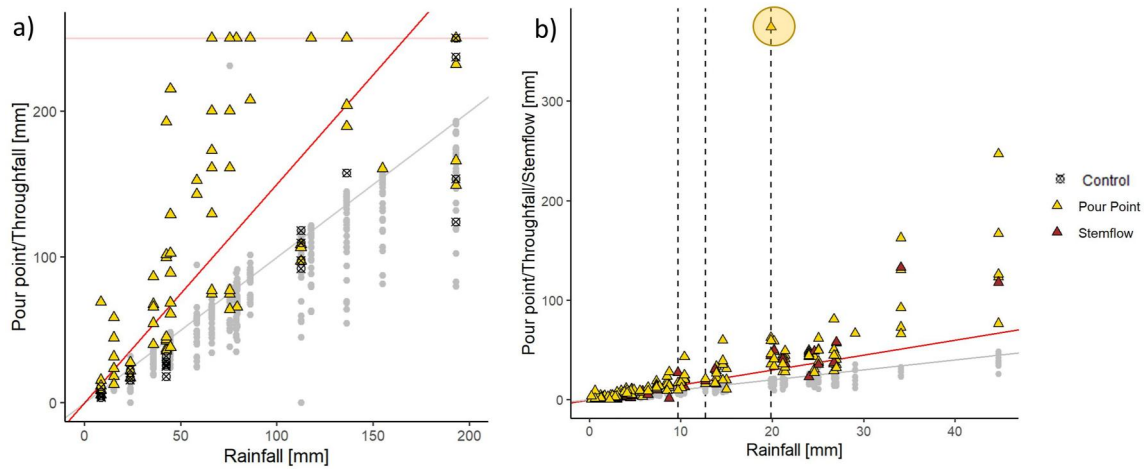

Figure 4. Pour points (indicated with the yellow triangle) consistently collected more water than throughfall gauges (gray circles) and stemflow (brown triangles). This was evident in the manual gauges (a) but with a limitation for the upper limit collected by the gauge at 250 mm (indicated with the orange line). This was not a problem with the automatic gauges (b) and allowed us to record extreme outliers as shown with the point highlighted. The 1:1 line is given in gray while the 1.5:1 line is given in red as a reference. The vertical dashed lines indicate the breakpoints for the pour points to rainfall regression.

Eleven of the pour points in the field were located in an area of 355 m^2 (area measured by a total station survey), approximately 1 pour point per 30 m^2. The search for pour points was not exhaustive, and this estimate is likely conservative: the site has approximately 1 tree per 26 m^2 and many of the instrumented trees contained at least two pour points. This intuition regarding the underestimation of number of pour points may be corroborated by the number of gauges that recorded depths of water $\geq 1.5 \times$ rainfall in the rainfall simulation experiments, as shown in Table 2. As the table shows, the branches that formed the pour point had, on average more than 1 pour point across a range of foliation conditions.

Combining the field and rainfall simulator cases, we found low rates of false positive pour point identification (1 in 20) and false negatives (1 in 6). The results suggest that pour points occur frequently, and can be reliably identified using visual inspection in the Banksia woodland.

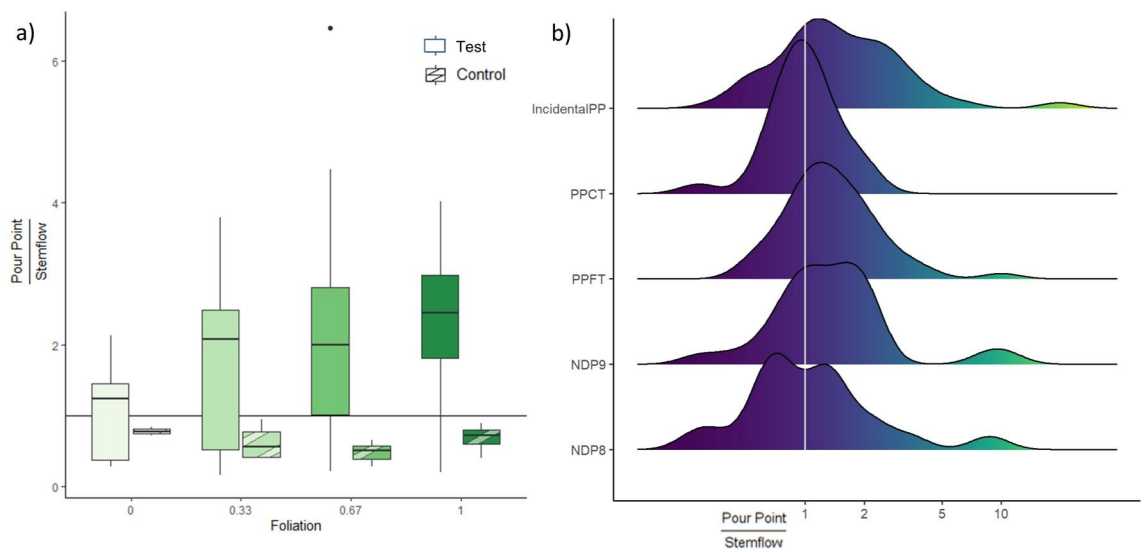

Figure 5. Pour point volume comparison with stemflow in (a) the rainfall simulation experiments and (b) the field. (a) Across the branches with measurable stemflow and the range of foliations, the pour point flux consistently exceeds stemflow (1:1 ratio is given by the horizontal black line), most evidently when compared with the control (see Section 2.3) (b) In the field, the distribution of the ratio of pour point volume to stemflow volume indicates that pour point fluxes also routinely exceed stemflow across all the automatic gauges (1:1 ratio is given by the vertical white line). (Note: in (b) the *x*-axis is logarithmic, and the *y*-axis has names of pour points listed in Table 1 and Section 3.1).

Table 2
Average Number of Gauges With More Than 1.5 Times Rainfall (Excluding Stemflow) for Different Foliation Conditions for Each Branchs

Branch	Full	2/3	1/3	0
*Br*1	4.25	1	1.67	1.4
*Br*3	0.625	0.33	0	0
*Br*4	1.8	1.8	0.5	0.67
*Br*5	5	4.75	3.2	1.25
GBT	6	2	4.167	0.75

Note. For example, *Br*1 Under Fully Foliated Conditions had 4 Trials. Across these 4 trials, 17 gauges recorded throughfall greater than 1.5. So then, on average there were 4.25 outliers for *Br*1 under fully foliated conditions).

3.2. Research Question 2: Could the Magnitude and Fate of Pour Point Fluxes Be Hydrologically Relevant?

3.2.1. Magnitude of Pour Point Fluxes

Pour points instrumented in the field recorded fluxes that were 1.5–15 times the rainfall flux. They were greater than throughfall as well, as shown in Figure 4a) on a per-reading basis for the manual gauges, and in Figure 4b), on a per-event basis for the tipping bucket gauges. The highest recorded ratio of pour point to rainfall was 15, (highlighted with a yellow circle in Figure 4b).

Figure 4b also shows three identified breakpoints in the rainfall-pour point regression at 10, 13, and 20 mm. The 13 and 20 mm breakpoints are influenced by the highlighted extreme outlier. The other breakpoint suggests that a change in slope when rainfall events exceed approximately 10 mm - potentially indicating the "activation" of high fluxes through the pour points for larger storms.

The depth of water delivered by the pour points was comparable to or in excess of stemflow in the rainfall simulation experiments and in the field. Figure 5 presents the ratio of pour point depth to stemflow depth for the rainfall simulation experiments across all foliation treatments (panel a) and the distribution of this ratio for all rainfall events measured in the field data (panel b, note the log scale on the horizontal axis). The median value of pour point to stemflow ratio exceeds 1 for all foliation conditions in the rainfall experiments simulations for the test branches but not the controls branch, suggesting that where pour point fluxes exist, they are comparable to or greater than stemflow fluxes in the banksia woodland.

Thus, the flux of water contained recorded underneath a pour point in the Banksia woodland is much higher than rainfall and background throughfall and is usually comparable to or greater than other commonly measured fluxes such as stemflow.

3.2.2. Fate of Pour Point Fluxes

More water infiltrated underneath all three instrumented pour points than the throughfall controls beside them. Figure 6a illustrates the time evolution of the difference in water content beneath the pour point and the control site over the course of a storm, at depths of 5, 22.5, and 100 cm below the soil surface. The rainfall timeseries is also shown. Figure 6a shows that more water arrives at the soil surface below a pour point than in adjacent areas, and that this difference in water content persists to depths of up to 1 m.

Infiltration at the pour points was 23%, 24%, and 33% of rainfall, while infiltration at the controls was 3%, 4%, and 17% of rainfall. At NDP1, the infiltration into the control point was considerably higher than the other 2 control points (as can be seen in Figure 6b). We are unclear if this represents an unaccounted-for pour/drip point, natural heterogeneity in infiltration, lateral preferential flow from the pour point site to the control, or another process: however it is evident that pour point versus control behavior was different at this location than the other instrumented sites. Infiltration at the other two pour points (NDP2 and NDP4), exceeded that at the controls by 94 and 151 mm, respectively, when accumulated over multiple storms (to a total depth of 497 mm).

Thus, the water from pour points appears to flow deeper in the soil and increase soil water storage inputs more than throughfall from nearby sites.

3.3. Research Question 3: What Are the Implications of Pour Point Formation for Measuring Throughfall and Closing the Canopy Water Balance?

3.3.1. Measuring Throughfall

The transformation of rainfall by the branches was clearly seen in the densely sampled throughfall field during the rainfall simulations. The spatial throughfall field for the fully foliated *Br*1 inclined 20° above horizontal from the natural angle is shown in Figure 7a illustrates the disparity between the pour point and all the other throughfall collected. It shows the highest ratio of pour point to rainfall flux recorded in the rainfall simulation experiments of 10. Figure 7b) contains data from the simulation where a fully foliated *GBT* was inclined 10° below horizontal

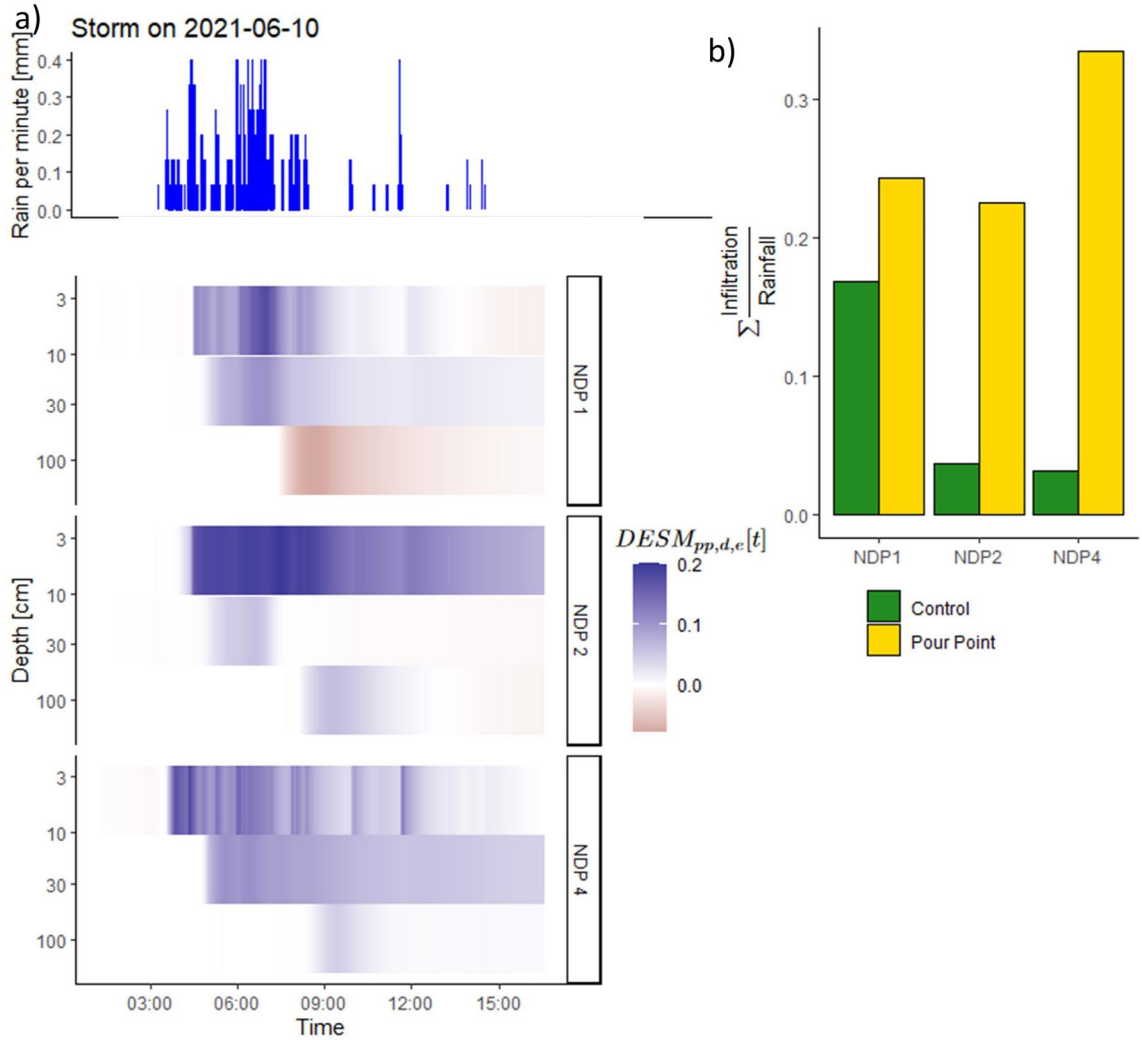

Figure 6. Soil moisture response to pour points. Panel (a) shows the difference in volumetric water content for the three instrumented pour points at the three depths for the storm plotted above the profiles. Note that the graph is indicative of the depth sampled; there were three soil moisture sensors at 5 cm, 22.5 cm, and 100 cm and the three distinct panels represent this. Panel (b) shows the ratio of infiltration to rainfall across the three pour points and the three controls.

from its natural angle. It shows the redistribution of rainfall from a homogeneous (white) field to areas of lower (red) and higher (blue) throughfall. This throughfall field shows that while the branch might create more modest pour point to rainfall ratios it creates several other potential pour or drip points.

This throughfall heterogeneity can be quantified with the CV in Table 3. Across all the trials, the CV of throughfall is 0.44, but if the pour points are excluded, the CV would be estimated as only 0.27 reducing the sampling requirements. Based on the commonly used throughfall sampling design (see Equation 7), an average of 110 gauges would be required to measure the mean throughfall within 10% of the mean, when pour points are considered and 46 if they are not. Table 3 shows that the heterogeneity in the measured throughfall declines with declining foliation across all branches. Overall, the presence of pour points greatly increases throughfall heterogeneity and, if randomized sampling designs were used, would greatly increase the sampling requirements for measuring throughfall fluxes, particularly for branches with more foliation.

3.3.2. Canopy Water Balance

The canopy water budget residuals for each branch across all experiments are shown in Figure 8a. The control branch (*Br*3), where there is no pour point, gives the least error (11% of rain received) and this error is not affected

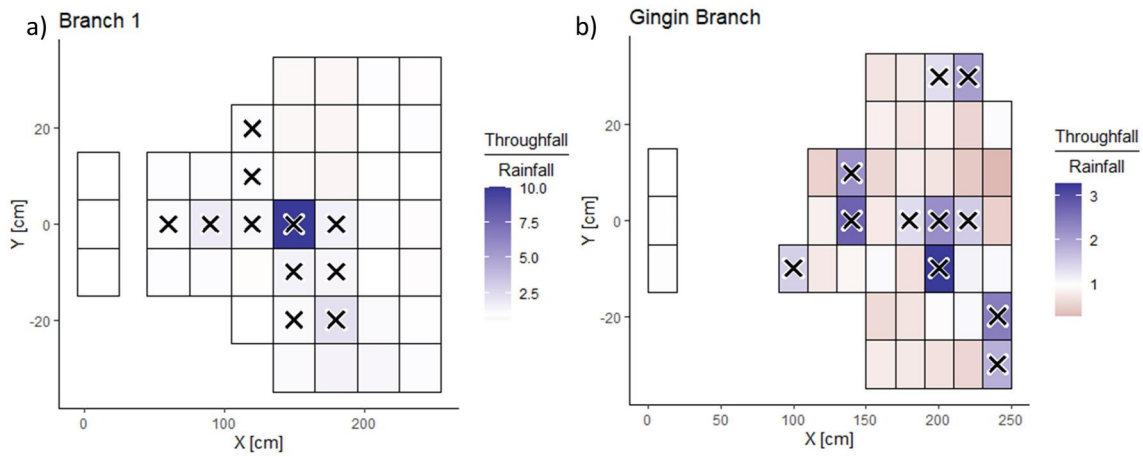

Figure 7. High spatial resolution of two throughfall fields for the branches shown in Figure 3. X indicated that the gauge was an outlier according to its *z* score. (a) *Br*1 had a sparser throughfall array. It recorded the highest pour point to rainfall ratio of 10, while the *GBT* (b) showed that there were several regions with greater throughfall than rainfall and even more with throughfall lower than rainfall. In both simulations, white coloration indicates no change in throughfall relative to rainfall and can be seen in the three control gauges.

substantially by the removal of pour points and stemflow (8% of rain received). This indicates that when there are no pour points, the existing design guidelines for randomized sampling and our sampling methodology produce reasonable results. The presence of pour points creates large water balance errors on all other branches (ranging from 59% to 243% of rain received), that are reduced by an order of magnitude (reduced to a range of −4 to 24% of rain received) if the pour point and stemflow gauges are excluded from the throughfall computation, and change sign if the other outlier gauges are also excluded.

Physically, these results indicate that more water appears in the throughfall gauges than was supplied as rainfall when a pour point was present—an impossible interpretation. On a per simulation basis, shown in Figure 8b), the ratio of the water balance residual to the total rainfall scales closely (see r^2 values in the caption) with the ratio of the pour point mass to the rainfall mass for each branch with a pour point, but with a different constant of proportionality for each branch. This suggests that pour points, and their unique relationship to individual branches, were responsible for the failure to close the water balance. The greater the volume of water received at the pour point, the worse was our ability to close the water balance for the rainfall simulations. The implication is that as the pour point flux increased, no corresponding decrease took place in the estimated throughfall—which would be needed to ensure water balance closure.

Thus, pour points confound the water balance closure if they are treated as just another throughfall measurement.

Table 3
Mean Values of Relevant Sampling Metrics for All the Branches Across Different Foliation

	All gauges				Without SF and PP				Without all outliers			
	CV		$n_{10\%}$		CV		$n_{10\%}$		CV		$n_{10\%}$	
Foliation	Test	Ctrl	Test	Ctrl	Test	Ctrl	Test	Ctrl	Test	Ctrl	Test	Ctrl
1	0.63	0.37	183	100	0.41	0.33	84	95	0.22	0.12	21	6
2/3	0.61	0.25	177	25	0.32	0.12	48	6	0.20	0.11	18	5
1/3	0.50	0.19	116	14	0.31	0.09	49	3	0.15	0.10	9	4
0	0.24	0.07	28	2	0.14	0.05	9	1	0.11	0.04	5	1

Note. Ctrl - the control branch. Test - values averaged for the remaining four branches. CV - coefficient of variation. $n_{10\%}$ - gauges required to estimate mean throughfall within 10% of the true mean.

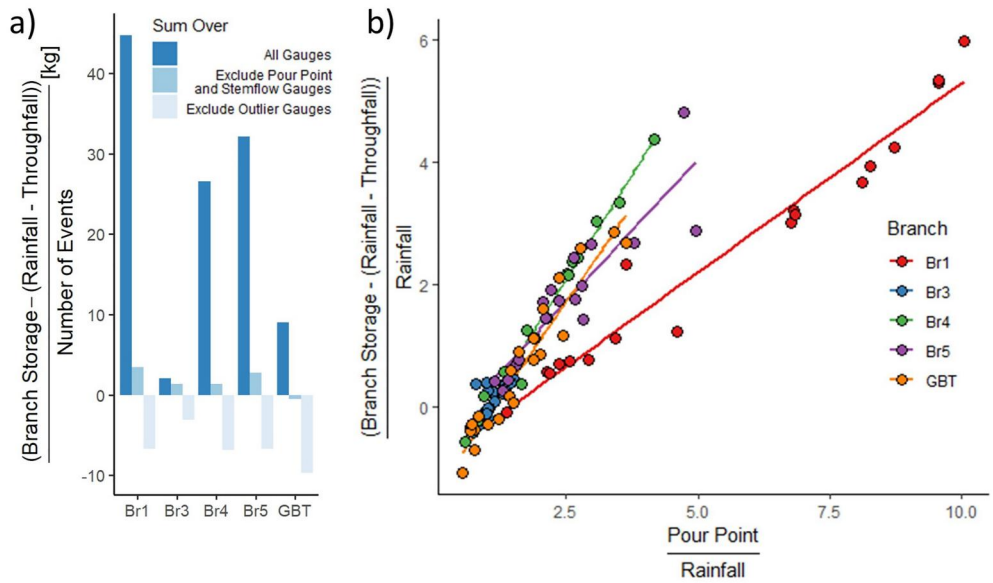

Figure 8. (a) The mean error in water balance closure for each branch across all the rainfall simulations using different gauges under the branch, (b) The ratio of error to rainfall as a function of pour point to rainfall ratio (each dot representing 1 simulation and each branch represented by a different color), the adjusted r^2 for $Br1 = 0.93$, the control branch $Br3 = 0.40$, $Br4 = 0.99$, $Br5 = 0.81$, and Gingin branch $GBT = 0.92$.

3.4. Research Question 4: How Do Branch Foliation and Angle Influence the Flux of Water Through Pour Points?

Variable relationships between foliation, branch angle and pour point formation or flux were identified in the simulations. For instance, while all branches formed more pour points when fully foliated than when the branch was baer (Table 2), 2 out of 5 branches produced more pour points at one third foliation than at two third foliation. The relationship between foliation and pour point fluxes was clearest for $Br1$. As shown in Figure 3a), $Br1$ had a large U bend that persistently formed a pour point. The flux of water moving through this pour point decreased with defoliation (Figure 9a)). However, no other branches had such a simple relationship between foliation and the pour point flux (Table 4).

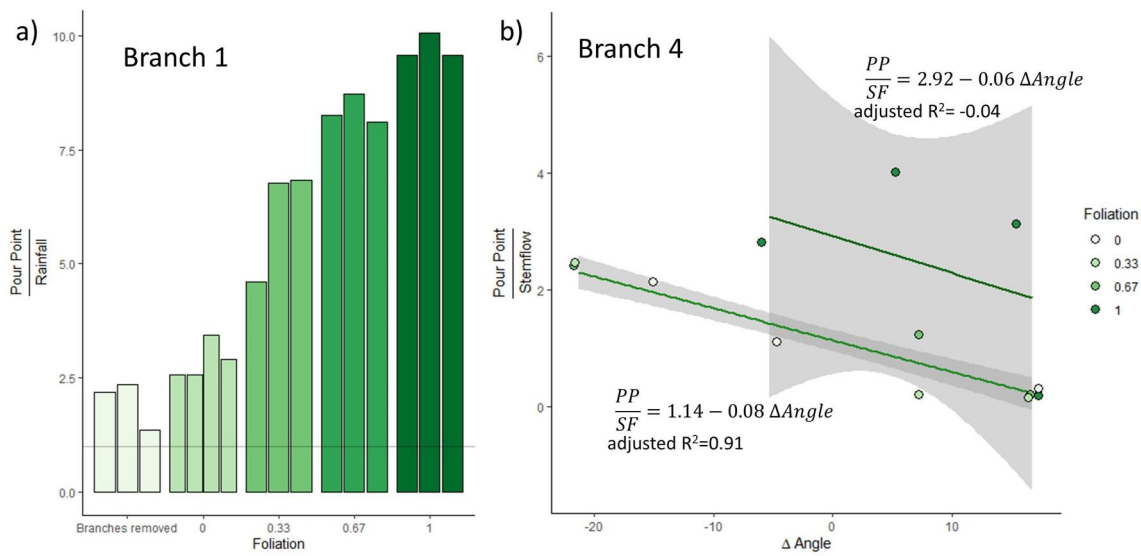

Figure 9. The influence of (a) foliation and (b) angle on the pour point. (a) Water received at the pour point for $Br1$ shows a clear decrease with foliation. For other branches such as (b) $Br4$, foliation and angle both played a part in the destination of water. The ratio of pour point flux to stemflow flux (PP/SF) decreased as the branch was made more vertical, that is as ΔAngle increased. The decrease was different for the fully foliated and the non-fully foliated branch.

Table 4
Adjusted R^2 *for the Linear Regression Models of Deviation of Pour Point to Rainfall Ratio From the Mean*

Branch	Foliation only	Angle only	Foliation and angle
*Br*1	0.62	0.06	0.56
*Br*3	−0.03	0.27	0.19
*Br*4	0.17	0.06	0.31
*Br*5	0.18	−0.03	0.12
GBT	0.12	−0.04	0.31

Pour point formation occurred differently on wet branches than dry. For example, the control branch did not form pour points when wet, but when dry a transient pour point was formed. As the branch became wetter this pour point migrated downgradient until it formed stemflow. The wetness of the branch was seen to be a precondition for water transport.

Branch angle also did not have a clear relationship with the normalized pour point depth, as indicated by the low adjusted r^2 values in Table 4. The variable and usually weak relationships between pour point flux, branch angle and leaf area suggest complex controls on the pour point dynamics. Similarly, only weak correlations arose between stemflow, foliation, and branch angle.

*Br*4 (see Figure 9b)) presents an interesting illustration of how foliation and angle can interact to alter the partitioning of water between stemflow and pour points. At full foliation, the pour point to stemflow ratio is high and insensitive to the change in angle (adjusted r^2 −0.121 for 5 instances). However, after a third of the leaves are removed, this ratio seems to be substantially influenced by angle (adjusted r^2 0.91 for 12 instances). Conceptually, as a branch is inclined more to the vertical, a greater component of gravity is accelerating the flow along the branch, facilitating the formation of stemflow rather than pour points. However, again, only one branch revealed such appealing and intuitive relations.

4. Discussion

4.1. Classification and Nomenclature

It is accepted that the rainfall intercepted by the canopy can be divided into throughfall, stemflow, and canopy interception loss. Further classification within throughfall is an emerging field (D. F. Levia et al., 2019), and we recognize that in using the term "pour points" we may be adding complexity. To clarify the terminology and classifications used, Figure 10 compares the classification of rainfall interception fluxes and processes by Nanko et al. (2022) with that used here. We assess these along the two fundamental dimensions of category systems (Rosch & Lloyd, 1978): vertical and horizontal. The vertical level represents the "inclusiveness of categories" and the horizontal the "segmentation of categories within the same level of inclusiveness" pg. 5 Rosch and

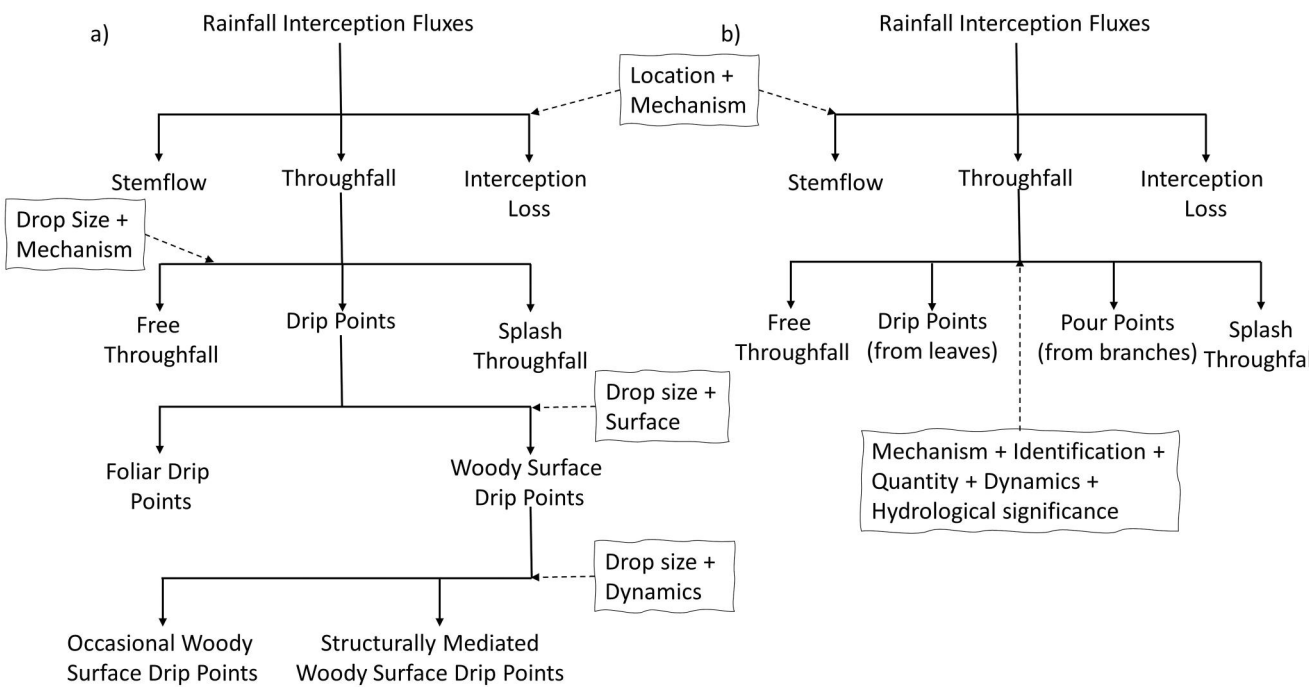

Figure 10. The nomenclature used in (a) Nanko et al. (2022) and (b) this study.

Lloyd (1978). Additionally, the two principles that govern whether a categorization is appropriate are the ease of information communication and the attributes that are used to distinguish the categories.

Nanko et al. (2022) developed their classifications based on drop size distribution and its timing. They inferred flow paths and residence times in the canopy from this drop data. In this scheme, structurally mediated woody surface drip points arise as a subset of drip points overall. This is a consequence of drop size being the attribute for inclusiveness and segmentation within these are based on the timing of drops (Rosch & Lloyd, 1978). For applications where drop sizes are of primary concern (Katayama et al., 2023), this category system is most appropriate.

Conversely, our classification separates drip points (throughfall readings that is are outliers falling from leaves) and pour points (throughfall readings that is are outliers falling from branches) based on flow mechanism, identification in the field, quantity of water conducted, dynamics of flow, and hydrological significance (Figure 10b). For example, the flow mechanisms on hydrophobic and flexible leaves (Holder, 2012; Rosado & Holder, 2013; Wang et al., 2020) are fundamentally different from those on generally hydrophilic stiff branches (Błońska et al., 2018; Herwitz, 1987). While rivulet flow occurs both, flow on leaves forms sessile rivulets (Towell & Rothfeld, 1966), compared to hanging, pendant rivulets flowing below branches (Indeikina et al., 1997). Drip points can be identified in the field with the help of leaf "drip tips" (Wang et al., 2020), while irregularities in branch architecture are needed to identify pour points (Herwitz, 1987). Pour points should be more persistent than drip points, as tree branch architecture changes more slowly than the leaf distribution. The network structure of tree canopies (Hallé et al., 2012) suggests that drip points should be more numerous. Leaves form the "zeroth order" (West et al., 1999) links of a convergent branch network (Bentley et al., 2013; Newman, 2018), and are generally numerous on trees. If leaves direct water to flow along a branch (Bialkowski & Buttle, 2015), pour points are likely to concentrate more flow than individual leaves. The difference between drip and pour points is also reflected in the literature about them: drip points have been studied quite extensively (Glass et al., 2010; Holder, 2012; Mayo et al., 2015; Wang et al., 2020; Xu et al., 2011; Yang et al., 2012), while pour points remain relatively (Nanko et al., 2022) uninvestigated. Consequently, separation of drip and pour points from mechanistic and hydrological perspectives, as per this study, offers its own advantages.

We do not suggest that at this point either classification mechanism is superior to the other, nor that there is necessarily a universally appropriate set of nomenclature to be adopted. Given the different aims and methodologies used to understand water partitioning by canopies, however, there is value in ongoing discussion amongst researchers to define useable and consistent terminologies.

4.2. Assessment of Pour Points in the Banksia Woodland

The field surveys and measurements indicated that pour points occurred in the Banksia woodland. They could be visually identified with high reliability, based on a combination of branch morphology, leaf area, staining/smoothing of the bark and splash marks on the soil surface. This identification system was developed by observing the woodland during a handful of rain events (see Movie S1). In the most heavily surveyed area, we identified pour points with an approximate density of one per 30 m^2 of Banksia woodland canopy—that is, approximately one per tree. We anticipate that this is an under-estimate, as our survey was not exhaustive, the rainfall simulations demonstrated several high flux points other than the identified pour point, and the false negative ratio was (1 in 6) greater than the false positive ratio (1 in 16) in the field instrumentation.

The magnitude of the water fluxes moving through pour points in the field was up to 15 times greater than rainfall and was almost always comparable to or greater than stemflow. It is important to note, that this magnitude was calculated as the ratio of volume and the collecting area of the gauge. If the gauge size changes this magnitude is going to change. Based on the magnitude calculated using the same gauges and the wide acceptance of stemflow as a hydrologically meaningful flux, these findings suggest that pour points merit hydrological consideration. Iida et al. (2018); D. F. Levia et al. (2020) show that at the high intensities observed at the pour points, there would be a greater need for dynamic calibration. While we only performed static calibrations in our study for the rain gauges, the undercatch increases as the intensity of water coming in increases, suggesting that we are likely underestimating the water directed toward the pour points.

Our subsurface measurements suggest that water flowing through pour points may travel deeper and produce wetter soils than throughfall or rainfall and may contribute to groundwater recharge. The 5 cm soil moisture

sensor indicated that the water received by the sensors below originated from the pour point. Rapid "Stage 1" evaporation is unlikely to occur (Or & Lehmann, 2019) when the wetting front travels below the 22.5 cm sensor. Lastly, once the wetting front passes the 1 m depth the water is unlikely to be extracted by half of the understorey species in the woodland (Groom et al., 2000) but may still be used by other species during dry periods (Veneklaas & Poot, 2003). Therefore, the water from the pour points moving deeper than these limits is likely to support the ecosystem rather than vaporizing from the soil directly (below 22.5 cm) or to ultimately contribute to recharge or deep soil moisture reserves (below 1 m) than rainfall or throughfall.

Measurements of throughfall and closure of canopy water balances from standard throughfall arrays are complicated by the presence of pour points. Pour points skew the distribution of throughfall by adding an extreme and non-random component. Ideally, pour points would be monitored deterministically, separately from attempts to capture the variation in the throughfall field through random sampling. The importance of such measurement strategies will vary with the frequency and magnitude of pour point fluxes but should form a consideration of hydrological sampling campaigns where morphological features or field observations suggest the presence of pour points.

The error in the water balance closure would suggest a physically impossible result of more flux of water following rather than before canopy interception. This was because the grid was designed to preferentially sample the pour point and therefore was not random. This requires complex statistics to resolve (Gelfand & Shirota, 2019) which can be an avenue for further research. Additionally, given the strong positive relationship between the concentration of water by the pour point and the error, it becomes clear that as the pour point concentrates greater rainfall, the decrease in the depths recorded at the throughfall gauges did not offset the increased depth in the pour point. Presumably, unsampled areas between the gauges contributed the water being recorded at the pour point. Troughs or gauges with larger surface areas might be helpful in reducing this error (A. Zimmermann & Zimmermann, 2014). Troughs however, generate some splash at the side walls, and need to be carefully designed and deployed (Reynolds & Neal, 1991). Sampling throughfall with troughs, would, additionally, obscure hydrologically relevant features of pour points, such as concentration of rain and increased heterogeneity that promote deeper infiltration.

Finally, the rainfall simulation experiments indicated that pour point fluxes could vary with the degree of foliation and the branch angle, but did not uncover consistent simple relationships between canopy architecture and the pour point flux. Iida et al. (2021) found inconsistent relationships between stemflow production and foliation as well. At present, variation in pour point fluxes for a constant rainfall intensity cannot be simply predicted as a linear function of foliation and branch angle. Qualitatively, we suggest that pour points form due to the branch carrying capacity, dictated by a branch architecture, being overwhelmed by amount of rain channeled by leaves.

4.3. Generalizing the Results

Several features of the Banksia woodland and Banksia canopies are likely to have made pour points prominent in this ecosystem. Banksia leaves are stiff, with a large surface area, and conduct water to the base of the leaves and then onto the branches rather than dripping off the leaf. Architecturally, *B. menziesii's* plagiotropic branches (Hallé et al., 2012) have a high degree of phototropism, meaning branches tend to "bend upwards" - creating changes in angle. Several new branches often emerge from a single point, generating confluences. These morphological features likely promote the formation of rivulet flow on branches and rivulet detachment as pour points.

At the land surface, the sandy soils have high hydraulic conductivity and very low water storage capacity, which both facilitate deep infiltration. This may have amplified the differences in infiltration behavior between pour points and throughfall relative to what would be observed on less conductive soils.

Despite the study site likely favoring pour point formation and a hydrological role for the pour points, the findings suggest that pour points should be generally considered in interception studies. Nanko et al. (2022) recorded structurally mediated woody surface drip points in a humid subtropical climate with American beech, yellow poplar red maple and oak, indicating that they are not unique to the Banksia woodland. Additionally, authors have observed this process on fig trees (*Ficus macrophylla*) in Western Australia. The behavior of pour points in the Banksia woodland emphasizes that plant canopies cause not only rainfall interception loss but also rainfall concentration and redistribution. This causes challenges for quantifying interception losses (Sadeghi et al., 2020), which are usually estimated as a residual of rainfall, throughfall, and stemflow without consideration of pour points as an additional concentration mechanism.

Measurement of representative throughfall fields in the presence of pour points is challenging, and likely requires deterministically sampling pour points, similarly to how stemflow is treated. Like stemflow, such measurements could then be used in physically based models (Davie & Durocher, 1997) to differentiate throughfall fluxes within the canopy and stemflow. However, optimal throughfall measurement designs where pour points occur need further investigation.

4.4. Future Work

While this study has defined pour points and established their potential hydrological relevance and associations with canopy architecture, key issues remain unresolved. First, without a more comprehensive survey relating pour point occurrence and fluxes to canopy area, upscaling the observations of pour points to determine their overall importance in the land surface water balance remains challenging. Pourpoints cannot be treated as just another throughfall reading. If 10 gauges were placed underneath a canopy and one recorded a pour point, then under a scenarios like the Banksia woodland where background throughfall is 0.80 rainfall and pour points may produce throughfall depths between 1.5 and 15 times rainfall, then the average throughfall estimates would vary from a reasonable 0.87 to a physically impossible 2.22 times rainfall. We have developed an interactive application which allows interested readers to see how these numbers may change for a different situations (Kunadi, 2023c).

Now consider, instead of depths of rainfall, the volumes of rainfall conveyed by pour points. We take two extremes of pour point density. The minimum density can be considered 1 pour point per 30 m^2 as seen in the area surveyed in the field. The maximum of ≈4 per 1.5 m^2 is derived from the average number of pour points across all the pour point branches in Table 4 when fully foliated. Assume that the rain gauge that recorded the pour point flux has an area of 0.02 m^2 and the pour point flux varied from 1.5 to 15 times rainfall. Under the conservative density, pour points would convey 0.1%–1% of total rain volume and under the maximum density, this would vary between 2% and 21%. Therefore, pour points could play a non-trivial role in the canopy water balance depending on their density and their rainfall concentration ability. Another interactive application has been developed for the reader to explore this relationship (Kunadi, 2023b). The influence of the size of the rain gauge collector area has on the estimate of the pour point discussed previously, is also shown in this app.

A key opportunity for future work would be conducting dedicated experiments to determine the subsurface fate of water from pour points. The method employed in the study allows for the comparison between pour point and control profiles, however methods like the 3D electrical resistivity tomography (Lowe et al., 2019) would allow for a richer understanding of the pour point flux beneath the soil surface. Alternatively, tracer techniques could be utilized. It is difficult to passively introduce a tracer into a naturally occurring pour point and it would be more straightforward to synthetically create traceable fluxes on branches by spraying dye (or isotopically distinct water) artificially. These could feasibly be used to trace synthetic pour points into the subsurface visually with dye, or potentially into vegetation or the groundwater using isotopes. Better understanding the interactions between canopy structure, throughfall concentration, and the fate of water in the landscape could improve land and water management (Filoso et al., 2017) and understanding of the critical zone (Brantley et al., 2007).

The understanding of flow mechanisms on the canopy could be substantially enhanced by the incorporation of drop size distribution that yielded the understanding of different flow paths (Nanko et al., 2022) and the biogeochemistry of the fluxes (Ponette-González et al., 2020). Consilience brought about by results from these different domains would offer certainty in our understanding of the rainfall interception process, while divergence would open rich domains for exploration. While, this study has proposed and used a certain nomenclature, practitioners incorporating these elements into their investigations should utilize the categorization framework (Figure 10) that they believe fits the attributes they are studying (Rosch & Lloyd, 1978).

The relationship of pour point concentration to controlled changes in rainfall intensity could not be investigated in this study. While the field experiments did offer data to explore this domain of study, the controlled rainfall simulation experiments were performed at a high intensity. The effect of this high intensity on pour point concentration of rainfall is unclear. We were able to obtain some clues from *GBT*: it recorded 15 times the rainfall depth in the field under natural conditions and a maximum of 3.6 times under the rainfall simulator. It may be hypothesized that the flowpaths leading to the pour point overflowed under the large quantity of water on the branch and the rivulets detached before the reached the pour point. Sophisticated rainfall simulators (Meena et al., 2022) that can recreate natural rainfall would be able to shed light on these findings and develop further insight.

Finally, the unclear relations between branch angle, foliation, and pour point behavior for the *B. menziesii* suggest that more careful analysis is needed to unpick what it is that changes in the interception and branch-flow generation processes as canopy morphology changes. A preliminary step, would be the study of this phenomenon on more species. Beyond that, utilizing canopy architecture to understanding stemflow has already generated some novel findings (Iida et al., 2021). Working on simplified systems (e.g., using pipes as simple analogs to branches) might offer opportunities for better-controlled experiments in which mechanisms are even more clearly elucidated. Advances in remote sensing and computer vision now offer exciting possibilities to rapidly image and interrogate the structure, connectivity, and surface characteristics of canopies (Gilani et al., 2017; Lau et al., 2018; Nouwakpo et al., 2016). Physical frameworks spanning percolation theory (Stauffer & Aharony, 2018), drop impact (Josserand & Thoroddsen, 2016), and rivulet flow (Alekseenko et al., 2008) on a porous surface (Alshaikhi et al., 2021) could be employed to predict the movement of water on and detachment from these surfaces. Pour points offer an opportunity to formulate and validate physical models of flow on the canopy.

5. Conclusion

Canopy interception of rainfall represents not only a process of water loss but also water concentration. Such concentration can produce large water fluxes that are distinct from conventional throughfall or stemflow when water detaches from a branch. This is termed a pour point. Such pour points have been shown to be prevalent, identifiable, and comparable or greater in water fluxes to stemflow in a Banksia woodland. They have unclear but definite relations to branch and canopy morphology, and pose challenges to the quantification of water inputs to the landscape in vegetated sites. Their importance in this water-limited seasonally-dry ecosystem was seen as they routed water deeper in the subsurface than throughfall and our observations suggest they represent a non-trivial component of rainfall volume. Thus, determining if pour points are present and adapting throughfall sampling strategies to their occurrence may be needed for an accurate understanding of water inputs to soils and ecosystems.

Further investigation of pour points and their production by canopies of varying morphology and surface properties opens up exciting potential opportunities to combine computer vision, mathematics, fluid mechanics, and hydrology to generate insight into the capacity of plant canopies to transform rainfall fluxes and modify the land surface water balance.

Data Availability Statement

The data used in this research has been uploaded to HydroShare database (Kunadi, 2023d) for open access and the code has been uploaded to GitHub and Zenodo (Kunadi, 2023a).

Acknowledgments
We would like to thank the two anonymous reviewers and Dr. Curtis D Holder for providing thorough reviews to the manuscript. Additionally, we'd like to thank Andrew Western and Andrew Guswa for examining a draft of this manuscript as a part of AK's thesis submission. This study has greatly benefited from the help of Carlos Ocampo, Kirsty Brooks, Andrew Van de ven, Xue Sen, and Hoang Long Nguyen. AK acknowledges UWA's support through a "Scholarship for International Research Fees and Ad Hoc Postgraduate Scholarship".

References

Alekseenko, S., Bobylev, A., & Markovich, D. (2008). Rivulet flow on the outer surface of an inclined cylinder. *Journal of Engineering and Thermophysics*, *17*(4), 259–272. https://doi.org/10.1134/s1810232808040012

Ali, R., McFarlane, D., Varma, S., Dawes, W., Emelyanova, I., Hodgson, G., & Charles, S. (2012). Potential climate change impacts on groundwater resources of south-western Australia. *Journal of Hydrology*, *475*, 456–472. https://doi.org/10.1016/j.jhydrol.2012.04.043

Allen, S. T., Aubrey, D. P., Bader, M. Y., Coenders-Gerrits, M., Friesen, J., Gutmann, E. D., et al. (2020). Key questions on the evaporation and transport of intercepted precipitation. In *Precipitation partitioning by vegetation* (pp. 269–280). Springer.

Alshaikhi, A. S., Wilson, S. K., & Duffy, B. R. (2021). Rivulet flow over and through a permeable membrane. *Physical Review Fluids*, *6*(10), 104003. https://doi.org/10.1103/physrevfluids.6.104003

Aschmann, H. (1973). Distribution and peculiarity of Mediterranean ecosystems. *Mediterranean Type Ecosystems: Origin and Structure*, *11–19*.

Aston, A. (1979). Rainfall interception by eight small trees. *Journal of hydrology*, *42*(3–4), 383–396. https://doi.org/10.1016/0022-1694(79)90057-x

Beczek, M., Ryżak, M., Lamorski, K., Sochan, A., Mazur, R., & Bieganowski, A. (2018). Application of x-ray computed microtomography to soil craters formed by raindrop splash. *Geomorphology*, *303*, 357–361. https://doi.org/10.1016/j.geomorph.2017.12.019

Bentley, L. P., Stegen, J. C., Savage, V. M., Smith, D. D., von Allmen, E. I., Sperry, J. S., et al. (2013). An empirical assessment of tree branching networks and implications for plant allometric scaling models. *Ecology Letters*, *16*(8), 1069–1078. https://doi.org/10.1111/ele.12127

Beringer, J., Hutley, L. B., McHugh, I., Arndt, S. K., Campbell, D., Cleugh, H. A., et al. (2016). An introduction to the Australian and New Zealand flux tower network–ozflux. *Biogeosciences*, *13*(21), 5895–5916. https://doi.org/10.5194/bg-13-5895-2016

Beringer, J., Moore, C. E., Cleverly, J., Campbell, D. I., Cleugh, H., De Kauwe, M. G., et al. (2022). Bridge to the future: Important lessons from 20 years of ecosystem observations made by the ozflux network. *Global Change Biology*, *28*(11), 3489–3514. https://doi.org/10.1111/gcb.16141

Bialkowski, R., & Buttle, J. (2015). Stemflow and throughfall contributions to soil water recharge under trees with differing branch architectures. *Hydrological Processes*, *29*(18), 4068–4082. https://doi.org/10.1002/hyp.10463

Błońska, E., Klamerus-Iwan, A., Łagan, S., & Lasota, J. (2018). Changes to the water repellency and storage of different species of deadwood based on decomposition rate in a temperate climate. *Ecohydrology*, *11*(8), e2023. https://doi.org/10.1002/eco.2023

Brantley, S. L., Goldhaber, M. B., & Ragnarsdottir, K. V. (2007). Crossing disciplines and scales to understand the critical zone. *Elements*, *3*(5), 307–314. https://doi.org/10.2113/gselements.3.5.307

Bulcock, H., & Jewitt, G. (2010). Spatial mapping of leaf area index using hyperspectral remote sensing for hydrological applications with a particular focus on canopy interception. *Hydrology and Earth System Sciences*, *14*(2), 383–392. https://doi.org/10.5194/hess-14-383-2010

Cavelier, J., Jaramillo, M., Solis, D., & de León, D. (1997). Water balance and nutrient inputs in bulk precipitation in tropical montane cloud forest in Panama. *Journal of Hydrology*, *193*(1–4), 83–96. https://doi.org/10.1016/s0022-1694(96)03151-4

Christiansen, J. E. (1942). *Irrigation by sprinkling* (Vol. 4). University of California Berkeley.

Cowling, R. M., Rundel, P. W., Lamont, B. B., Arroyo, M. K., & Arianoutsou, M. (1996). Plant diversity in Mediterranean-climate regions. *Trends in Ecology & Evolution*, *11*(9), 362–366. https://doi.org/10.1016/0169-5347(96)10044-6

Crockford, R., & Richardson, D. (1990). Partitioning of rainfall in a eucalypt forest and pine plantation in southeastern Australia: II stemflow and factors affecting stemflow in a dry sclerophyll eucalypt forest and a pinus radiata plantation. *Hydrological Processes*, *4*(2), 145–155. https://doi.org/10.1002/hyp.3360040205

Davie, T., & Durocher, M. (1997). A model to consider the spatial variability of rainfall partitioning within deciduous canopy. I. model description. *Hydrological Processes*, *11*(11), 1509–1523. https://doi.org/10.1002/(sici)1099-1085(199709)11:11<1509::aid-hyp482>3.3.co;2-c

Dralle, D. N., Hahm, W. J., Rempe, D. M., Karst, N., Anderegg, L. D., Thompson, S. E., et al. (2020). Plants as sensors: Vegetation response to rainfall predicts root-zone water storage capacity in Mediterranean-type climates. *Environmental Research Letters*, *15*(10), 104074. https://doi.org/10.1088/1748-9326/abb10b

Dunkerley, D. (2020). A review of the effects of throughfall and stemflow on soil properties and soil erosion. In *Precipitation partitioning by vegetation* (pp. 183–214). Springer.

Eroglu, D., McRobie, F. H., Ozken, I., Stemler, T., Wyrwoll, K.-H., Breitenbach, S. F., et al. (2016). See–saw relationship of the Holocene East Asian–Australian summer monsoon. *Nature Communications*, *7*(1), 1–7. https://doi.org/10.1038/ncomms12929

Filoso, S., Bezerra, M. O., Weiss, K. C., & Palmer, M. A. (2017). Impacts of forest restoration on water yield: A systematic review. *PLoS One*, *12*(8), e0183210. https://doi.org/10.1371/journal.pone.0183210

Ford, E., & Deans, J. (1978). The effects of canopy structure on stemflow, throughfall and interception loss in a young Sitka spruce plantation. *Journal of Applied Ecology*, *915*(3), 905. https://doi.org/10.2307/2402786

Garcia-Estringana, P., Alonso-Blázquez, N., & Alegre, J. (2010). Water storage capacity, stemflow and water funneling in Mediterranean shrubs. *Journal of Hydrology*, *389*(3–4), 363–372. https://doi.org/10.1016/j.jhydrol.2010.06.017

Garnier, S., Ross, N., Rudis, R., Camargo, P. A., Sciaini, M., & Scherer, C. (2021). viridis - Colorblind-friendly color maps for r (R package version 0.6.2) [Computer software manual]. Zenodo. https://doi.org/10.5281/zenodo.4679424

Geißler, C., Kühn, P., Böhnke, M., Bruelheide, H., Shi, X., & Scholten, T. (2012). Splash erosion potential under tree canopies in subtropical se China. *Catena*, *91*, 85–93. https://doi.org/10.1016/j.catena.2010.10.009

Gelfand, A. E., & Shirota, S. (2019). Preferential sampling for presence/absence data and for fusion of presence/absence data with presence-only data. *Ecological Monographs*, *89*(3), e01372. https://doi.org/10.1002/ecm.1372

Genton, M. G. (1998). Highly robust variogram estimation. *Mathematical Geology*, *30*(2), 213–221. https://doi.org/10.1023/a:1021728614555

Gilani, S. Z., Mian, A., Shafait, F., & Reid, I. (2017). Dense 3D face correspondence. *IEEE Transactions on Pattern Analysis and Machine Intelligence*, *40*(7), 1584–1598. https://doi.org/10.1109/tpami.2017.2725279

Glass, R. C., Walters, K. F., Gaskell, P. H., Lee, Y. C., Thompson, H. M., Emerson, D. R., & Gu, X.-J. (2010). Recent advances in computational fluid dynamics relevant to the modelling of pesticide flow on leaf surfaces. *Pest Management Science: Formerly Pesticide Science*, *66*(1), 2–9. https://doi.org/10.1002/ps.1824

Grolemund, G., & Wickham, H. (2011). Dates and times made easy with lubridate. *Journal of Statistical Software*, *40*(3), 1–25. https://doi.org/10.18637/jss.v040.i03

Groom, B. P. K., Froend, R. H., & Mattiske, E. M. (2000). Impact of groundwater abstraction on a banksia woodland, swan coastal plain, Western Australia. *Ecological Management and Restoration*, *1*(2), 117–124. https://doi.org/10.1046/j.1442-8903.2000.00033.x

Guswa, A. J., & Spence, C. M. (2012). Effect of throughfall variability on recharge: Application to hemlock and deciduous forests in western Massachusetts. *Ecohydrology*, *5*(5), 563–574. https://doi.org/10.1002/eco.281

Hallé, F., Oldeman, R. A., & Tomlinson, P. B. (2012). *Tropical trees and forests: An architectural analysis*. Springer Science & Business Media.

Herwitz, S. R. (1987). Raindrop impact and water flow on the vegetative surfaces of trees and the effects on stemflow and throughfall generation. *Earth Surface Processes and Landforms*, *12*(4), 425–432. https://doi.org/10.1002/esp.3290120408

Holder, C. D. (2012). The relationship between leaf hydrophobicity, water droplet retention, and leaf angle of common species in a semi-arid region of the western United States. *Agricultural and Forest Meteorology*, *152*, 11–16. https://doi.org/10.1016/j.agrformet.2011.08.005

Holwerda, F., Scatena, F., & Bruijnzeel, L. (2006). Throughfall in a Puerto Rican lower montane rain forest: A comparison of sampling strategies. *Journal of Hydrology*, *327*(3–4), 592–602. https://doi.org/10.1016/j.jhydrol.2005.12.014

Iida, S., Levia, D. F., Nanko, K., Sun, X., Shimizu, T., Tamai, K., & Shinohara, Y. (2018). Correction of canopy interception loss measurements in temperate forests: A comparison of necessary adjustments among three different rain gauges based on a dynamic calibration procedure. *Journal of Hydrometeorology*, *19*(3), 547–553. https://doi.org/10.1175/jhm-d-17-0124.1

Iida, S., Wheeler, K. I., Nanko, K., Shinohara, Y., Sun, X., Sakai, N., & Levia, D. F. (2021). Canopy structure metrics governing stemflow funnelling differ between leafed and leafless states: Insights from a large-scale rainfall simulator. *Hydrological Processes*, *35*(8), e14294. https://doi.org/10.1002/hyp.14294

Indeikina, A., Veretennikov, I., & Chang, H.-C. (1997). Drop fall-off from pendent rivulets. *Journal of Fluid Mechanics*, *338*, 173–201. https://doi.org/10.1017/s0022112096004879

Johnson, M. S., & Lehmann, J. (2006). Double-funneling of trees: Stemflow and root-induced preferential flow. *Écoscience*, *13*(3), 324–333. https://doi.org/10.2980/i1195-6860-13-3-324.1

Josserand, C., & Thoroddsen, S. T. (2016). Drop impact on a solid surface. *Annual Review of Fluid Mechanics*, *48*(1), 365–391. https://doi.org/10.1146/annurev-fluid-122414-034401

Katayama, A., Nanko, K., Jeong, S., Kume, T., Shinohara, Y., & Seitz, S. (2023). Concentrated impacts by tree canopy drips: Hotspots of soil erosion in forests. *Earth surface dynamics discussions* (pp.1–12).

Keim, R. F., Skaugset, A., & Weiler, M. (2006). Storage of water on vegetation under simulated rainfall of varying intensity. *Advances in Water Resources*, *29*(7), 974–986. https://doi.org/10.1016/j.advwatres.2005.07.017

Keim, R. F., Skaugset, A. E., & Weiler, M. (2005). Temporal persistence of spatial patterns in throughfall. *Journal of Hydrology*, *314*(1–4), 263–274. https://doi.org/10.1016/j.jhydrol.2005.03.021

Kimmins, J. (1973). Some statistical aspects of sampling throughfall precipitation in nutrient cycling studies in British Columbian coastal forests. *Ecology*, *54*(5), 1008–1019. https://doi.org/10.2307/1935567
Kunadi, A. S. (2023a). Pour Point Code: v1.0.0 [Software]. Zenodo. https://doi.org/10.5281/zenodo.10333812
Kunadi, A. S. (2023b). Total Pour Point Flux: v1.0.0 [Software]. Zenodo. https://doi.org/10.5281/zenodo.10333829
Kunadi, A. S. (2023c). Ratio of pour points [Software]. Zenodo. https://doi.org/10.5281/zenodo.10333863
Kunadi, A. S. (2023d). Quantifying pour points: Throughfall concentration measured in the field and in rainfall simulations [Dataset]. HydroShare. Retrieved from http://www.hydroshare.org/resource/44394ab04f7040e4a5afdff376265e5d
Lau, A., Bentley, L. P., Martius, C., Shenkin, A., Bartholomeus, H., Raumonen, P., et al. (2018). Quantifying branch architecture of tropical trees using terrestrial lidar and 3D modelling. *Trees*, *32*(5), 1219–1231. https://doi.org/10.1007/s00468-018-1704-1
Levia, D., Michalzik, B., Näthe, K., Bischoff, S., Richter, S., & Legates, D. (2015). Differential stemflow yield from European beech saplings: The role of individual canopy structure metrics. *Hydrological Processes*, *29*(1), 43–51. https://doi.org/10.1002/hyp.10124
Levia, D. F., Carlyle-Moses, D. E., Michalzik, B., Nanko, K., & Tischer, A. (2020). *Forest-water interactions* (Vol. 240). Springer.
Levia, D. F., & Germer, S. (2015). A review of stemflow generation dynamics and stemflow-environment interactions in forests and shrublands. *Reviews of Geophysics*, *53*(3), 673–714. https://doi.org/10.1002/2015rg000479
Levia, D. F., Hudson, S. A., Llorens, P., & Nanko, K. (2017). Throughfall drop size distributions: A review and prospectus for future research. *Wiley Interdisciplinary Reviews: Water*, *4*(4), e1225. https://doi.org/10.1002/wat2.1225
Levia, D. F., Jr., & Frost, E. E. (2006). Variability of throughfall volume and solute inputs in wooded ecosystems. *Progress in Physical Geography*, *30*(5), 605–632. https://doi.org/10.1177/0309133306071145
Levia, D. F., Nanko, K., Amasaki, H., Giambelluca, T. W., Hotta, N., Iida, S., et al. (2019). Throughfall partitioning by trees. *Hydrological Processes*, *33*(12), 1698–1708. https://doi.org/10.1002/hyp.13432
Li, X., Xiao, Q., Niu, J., Dymond, S., van Doorn, N. S., Yu, X., et al. (2016). Process-based rainfall interception by small trees in northern China: The effect of rainfall traits and crown structure characteristics. *Agricultural and Forest Meteorology*, *218*, 65–73. https://doi.org/10.1016/j.agrformet.2015.11.017
Liang, W.-L. (2020). *Effects of stemflow on soil water dynamics in forest stands* (pp. 349–370). Forest-water interactions.
Lloyd, C. R., & Marques, F. A. O. (1988). Spatial variability of throughfall and stemflow measurements in Amazonian rainforest. *Agricultural and Forest Meteorology*, *42*(1), 63–73. https://doi.org/10.1016/0168-1923(88)90067-6
Loadcell Supplies. (2010). Model DBBP series. Retrieved from https://loadcell.com.au/products/loadcells/bongshin-dbbp/?attachment_id=1558&download_file=5cfro66is86qi
Lotsch, A., Friedl, M. A., Anderson, B. T., & Tucker, C. J. (2003). Coupled vegetation-precipitation variability observed from satellite and climate records. *Geophysical Research Letters*, *30*(14), 1774. https://doi.org/10.1029/2003gl017506
Lowe, M.-A. (2019). *Soil water repellency and its limitations on water infiltration (Unpublished doctoral dissertation)*. University of Western Australia.
Lowe, M.-A., Mathes, F., Loke, M. H., McGrath, G., Murphy, D. V., & Leopold, M. (2019). Bacillus subtilis and surfactant amendments for the breakdown of soil water repellency in a sandy soil. *Geoderma*, *344*, 108–118. https://doi.org/10.1016/j.geoderma.2019.02.038
Martinez-Meza, E., & Whitford, W. G. (1996). Stemflow, throughfall and channelization of stemflow by roots in Three Chihuahuan desert shrubs. *Journal of Arid Environments*, *32*(3), 271–288.
Mayo, L. C., McCue, S. W., Moroney, T. J., Forster, W. A., Kempthorne, D. M., Belward, J. A., & Turner, I. W. (2015). Simulating droplet motion on virtual leaf surfaces. *Royal Society Open Science*, *2*(5), 140528. https://doi.org/10.1098/rsos.140528
Mazur, R., Ryżak, M., Sochan, A., Beczek, M., Polakowski, C., Przysucha, B., & Bieganowski, A. (2022). Soil deformation after one water-drop impact–the effect of texture and soil moisture content. *Geoderma*, *417*, 115838. https://doi.org/10.1016/j.geoderma.2022.115838
Meena, R. K., Sen, S., Nanda, A., Dass, B., & Mishra, A. (2022). A contribution to rainfall simulator design–a concept of moving storm automation. *Hydrology and Earth System Sciences*, *26*(16), 4379–4390. https://doi.org/10.5194/hess-26-4379-2022
Muzylo, A., Llorens, P., Valente, F., Keizer, J., Domingo, F., & Gash, J. (2009). A review of rainfall interception modelling. *Journal of hydrology*, *370*(1–4), 191–206. https://doi.org/10.1016/j.jhydrol.2009.02.058
Nanko, K., Hudson, S. A., & Levia, D. F. (2016). Differences in throughfall drop size distributions in the presence and absence of foliage. *Hydrological Sciences Journal*, *61*(3), 620–627. https://doi.org/10.1080/02626667.2015.1052454
Nanko, K., Keim, R. F., Hudson, S. A., & Levia, D. F. (2022). Throughfall drop sizes suggest canopy flowpaths vary by phenophase. *Journal of Hydrology*, *612*, 128144. https://doi.org/10.1016/j.jhydrol.2022.128144
Návar, J. (2011). Stemflow variation in Mexico's northeastern forest communities: Its contribution to soil moisture content and aquifer recharge. *Journal of Hydrology*, *408*(1–2), 35–42. https://doi.org/10.1016/j.jhydrol.2011.07.006
Newman, M. (2018). *Networks*. Oxford university press.
Nouwakpo, S. K., Weltz, M. A., & McGwire, K. (2016). Assessing the performance of structure-from-motion photogrammetry and terrestrial lidar for reconstructing soil surface microtopography of naturally vegetated plots. *Earth Surface Processes and Landforms*, *41*(3), 308–322. https://doi.org/10.1002/esp.3787
Nulsen, R., Bligh, K., Baxter, I., Solin, E., & Imrie, D. (1986). The fate of rainfall in a mallee and heath vegetated catchment in southern western Australia. *Australian Journal of Ecology*, *11*(4), 361–371. https://doi.org/10.1111/j.1442-9993.1986.tb01406.x
Or, D., & Lehmann, P. (2019). Surface evaporative capacitance: How soil type and rainfall characteristics affect global-scale surface evaporation. *Water Resources Research*, *55*(1), 519–539. https://doi.org/10.1029/2018wr024050
Ponette-González, A. G., Van Stan, J. T., II, & Magyar, D. (2020). Things seen and unseen in throughfall and stemflow. In *Precipitation partitioning by vegetation* (pp. 71–88). Springer.
QGIS Development Team. (2022). QGIS geographic information system. Retrieved from https://www.qgis.org
R Core Team. (2018). R: A language and environment for statistical computing. Retrieved from https://www.R-project.org/
Reynolds, B., & Neal, C. (1991). Trough versus funnel collectors for measuring throughfall volumes. *Journal of Environmental Quality*, *20*(3), 518–521. https://doi.org/10.2134/jeq1991.00472425002000030003x
Rosado, B. H., & Holder, C. D. (2013). The significance of leaf water repellency in ecohydrological research: A review. *Ecohydrology*, *6*(1), 150–161. https://doi.org/10.1002/eco.1340
Rosch, E., & Lloyd, B. B. (1978). Cognition and categorization.
Rousseeuw, P. J., & Hubert, M. (2011). Robust statistics for outlier detection. *Wiley Interdisciplinary Reviews: Data Mining and Knowledge Discovery*, *1*(1), 73–79. https://doi.org/10.1002/widm.2
Rutter, A. (1963). Studies in the water relations of pinus sylvestris in plantation conditions I. measurements of rainfall and interception. *Journal of Ecology*, *51*(1), 191–203. https://doi.org/10.2307/2257513

Rye, C., & Smettem, K. (2017). The effect of water repellent soil surface layers on preferential flow and bare soil evaporation. *Geoderma*, *289*, 142–149. https://doi.org/10.1016/j.geoderma.2016.11.032

Sadeghi, S. M. M., Gordon, D. A., & Van Stan, J. T., II. (2020). A global synthesis of throughfall and stemflow hydrometeorology. In *Precipitation partitioning by vegetation* (pp. 49–70). Springer.

Salama, R. B., Silberstein, R., & Pollock, D. (2005). Soils characteristics of the bassendean and spearwood sands of the Gnangara mound (western Australia) and their controls on recharge, water level patterns and solutes of the superficial aquifer. *Water, Air, and Soil Pollution: Focus*, *5*(1), 3–26. https://doi.org/10.1007/s11267-005-7396-8

Silberstein, R. (2015). Gingin ozflux: Australian and New Zealand flux research and monitoring.

Skurray, J. H., Roberts, E., & Pannell, D. J. (2012). Hydrological challenges to groundwater trading: Lessons from south-west western Australia. *Journal of hydrology*, *412*, 256–268. https://doi.org/10.1016/j.jhydrol.2011.05.034

Staelens, J., Herbst, M., Hölscher, D., & Schrijver, A. D. (2011). Seasonality of hydrological and biogeochemical fluxes. In *Forest hydrology and biogeochemistry* (pp. 521–539). Springer.

Stan, J. T. V., Hildebrandt, A., Friesen, J., Metzger, J. C., & Yankine, S. A. (2020). Spatial variability and temporal stability of local net precipitation patterns. *Precipitation partitioning by vegetation* (pp. 89–104). https://doi.org/10.1007/978-3-030-29702-2_6

Stauffer, D., & Aharony, A. (2018). *Introduction to percolation theory*. Taylor & Francis.

Taniguchi, M., Tsujimura, M., & Tanaka, T. (1996). Significance of stemflow in groundwater recharge. 1: Evaluation of the stemflow contribution to recharge using a mass balance approach. *Hydrological Processes*, *10*(1), 71–80. https://doi.org/10.1002/(sici)1099-1085(199601)10:1<71::aid-hyp301>3.0.co;2-q

Thompson, S., Harman, C., Heine, P., & Katul, G. (2010a). Vegetation-infiltration relationships across climatic and soil type gradients. *Journal of Geophysical Research*, *115*(G2), G02023. https://doi.org/10.1029/2009jg001134

Thompson, S. E., Katul, G. G., & Porporato, A. (2010b). Role of microtopography in rainfall-runoff partitioning: An analysis using idealized geometry. *Water Resources Research*, *46*(7), W07520. https://doi.org/10.1029/2009wr008835

Towell, G., & Rothfeld, L. (1966). Hydrodynamics of rivulet flow. *AIChE Journal*, *12*(5), 972–980. https://doi.org/10.1002/aic.690120524

Tucker, A., Levia, D. F., Katul, G. G., Nanko, K., & Rossi, L. F. (2020). A network model for stemflow solute transport. *Applied Mathematical Modelling*, *88*, 266–282. https://doi.org/10.1016/j.apm.2020.06.047

Turner, B. L., & Laliberte, E. (2020). Proposal for a new bassendean reference soil in western Australia. *Journal of the Royal Society of Western Australia*, *103*, 1–8.

Van Elewijck, L. (1989). Influence of leaf and branch slope on stemflow amount. *Catena*, *16*(4–5), 525–533. https://doi.org/10.1016/0341-8162(89)90033-7

van Meerveld, H., Jones, J. P., Ghimire, C. P., Zwartendijk, B. W., Lahitiana, J., Ravelona, M., & Mulligan, M. (2021). Forest regeneration can positively contribute to local hydrological ecosystem services: Implications for forest landscape restoration. *Journal of Applied Ecology*, *58*(4), 755–765. https://doi.org/10.1111/1365-2664.13836

Van Stan, J. T., Gutmann, E., & Friesen, J. (2020). *Precipitation partitioning by vegetation: A global synthesis*. Springer Nature.

Veneklaas, E. J., & Poot, P. (2003). Seasonal patterns in water use and leaf turnover of different plant functional types in a species-rich woodland, south-western Australia. *Plant and Soil*, *257*(2), 295–304. https://doi.org/10.1023/a:1027383920150

Viola, F., Daly, E., Vico, G., Cannarozzo, M., & Porporato, A. (2008). Transient soil-moisture dynamics and climate change in Mediterranean ecosystems. *Water Resources Research*, *44*(11). https://doi.org/10.1029/2007wr006371

Wang, T., Si, Y., Dai, H., Li, C., Gao, C., Dong, Z., & Jiang, L. (2020). Apex structures enhance water drainage on leaves. *Proceedings of the National Academy of Sciences*, *117*(4), 1890–1894. https://doi.org/10.1073/pnas.1909924117

West, G. B., Brown, J. H., & Enquist, B. J. (1999). The fourth dimension of life: Fractal geometry and allometric scaling of organisms. *Science*, *284*(5420), 1677–1679. https://doi.org/10.1126/science.284.5420.1677

Whelan, M., & Anderson, J. (1996). Modelling spatial patterns of throughfall and interception loss in a Norway spruce (picea abies) plantation at the plot scale. *Journal of Hydrology*, *186*(1–4), 335–354. https://doi.org/10.1016/s0022-1694(96)03020-x

Wickham, H. (2007). Reshaping data with the reshape package. *Journal of Statistical Software*, *21*(12), 1–20. https://doi.org/10.18637/jss.v021.i12

Wickham, H. (2016). *ggplot2: Elegant graphics for data analysis*. Springer-Verlag New York. Retrieved from https://ggplot2.tidyverse.org

World Bank. (2022a). Forest land (% of land area). Retrieved from https://data.worldbank.org/indicator/AG.LND.AGRI.ZS

World Bank. (2022b). Agricultural land (% of land area). Retrieved from https://data.worldbank.org/indicator/AG.LND.FRST.ZS

Xiao, Q., & McPherson, E. G. (2016). Surface water storage capacity of twenty tree species in Davis, California. *Journal of Environmental Quality*, *45*(1), 188–198. https://doi.org/10.2134/jeq2015.02.0092

Xu, L., Zhu, H., Ozkan, H. E., Bagley, W. E., & Krause, C. R. (2011). Droplet evaporation and spread on waxy and hairy leaves associated with type and concentration of adjuvants. *Pest Management Science*, *67*(7), 842–851. https://doi.org/10.1002/ps.2122

Yang, M., Jiang, L., Li, X., Liu, Y., Liu, X., & Wu, E. (2012). Interactive coupling between a tree and raindrops. *Computer Animations and Virtual Worlds*, *23*(3–4), 267–277. https://doi.org/10.1002/cav.1451

Zeileis, A., Kleiber, C., Krämer, W., & Hornik, K. (2003). Testing and dating of structural changes in practice. *Computational Statistics & Data Analysis*, *44*(1–2), 109–123. https://doi.org/10.1016/S0167-9473(03)00030-6

Zeileis, A., Leisch, F., Hornik, K., & Kleiber, C. (2002). strucchange: An r package for testing for structural change in linear regression models. *Journal of Statistical Software*, *7*(2), 1–38. https://doi.org/10.18637/jss.v007.i02

Zimmermann, A., & Zimmermann, B. (2014). Requirements for throughfall monitoring: The roles of temporal scale and canopy complexity. *Agricultural and Forest Meteorology*, *189*, 125–139. https://doi.org/10.1016/j.agrformet.2014.01.014

Zimmermann, A., Zimmermann, B., & Elsenbeer, H. (2009). Rainfall redistribution in a tropical forest: Spatial and temporal patterns. *Water Resources Research*, *45*(11), W11413. https://doi.org/10.1029/2008wr007470

Zimmermann, B., Zimmermann, A., Lark, R. M., & Elsenbeer, H. (2010). Sampling procedures for throughfall monitoring: A simulation study. *Water Resources Research*, *46*(1), W01503. https://doi.org/10.1029/2009wr007776